GEOTECHNICAL ENGINEERING PROJECT DAY 2019

A Presentation of Best Geotechnical Engineering Undergraduate Projects in Sri Lankan Universities

11th June, 2019
At Faculty of Engineering
University of Ruhuna Auditorium

Organised by the
SRI LANKAN GEOTECHNICAL SOCIETY

SLGS

GEOTECHNICAL ENGINEERING
PROJECT DAY – 2019

Message from the President - SLGS

From its inception, Sri Lankan Geotechnical Society has provided a forum for disseminating new knowledge in the field of geotechnical engineering and promoting research. It has organized many conferences, workshops and field visits in this context.

The Project Day competition is an annual event held among Sri Lankan undergraduates doing projects in the field of geotechnical engineering. It commenced in year 2000 with the objective of encouraging them to do good research and publish. Participants are expected to present their findings in a concise four paged paper and make a 15-minute oral presentation. The best paper and the second paper will receive cash awards and certificates.

Many winners in the past years have proceeded to do higher studies and established good carriers in the field of Geotechnical Engineering as both academics and practicing engineers.

It is encouraging to note that there are eleven papers on a wide variety of topics this year. I thank all the authors for their interest and commitment and hope they will continue with the habit of presenting their research in written form. It is only when one starts to write his findings, he would realize the gaps in his work or knowledge and would be able to rectify them.

I also wish to convey my sincere gratitude to the panel of evaluators; Prof. U. G. A. Puswewala, Dr. J. J. P. Ameratunga and Dr. J. S. M. Fowze.

Prof. Athula Kulathilaka
President – SLGS

CONTENTS

Establishment of Soil Water Characteristic Curves (SWCC) for Sri Lankan Residual Soils

K.K.D. Dhananjaya
Department of Civil Engineering, University of Moratuwa, Sri Lanka

ABSTRACT: Rain induced slope failures are a major challenge in Sri Lanka. Soil Water Characteristic Curve (SWCC) is essential in modelling the destruction of matric suction by infiltration of rainwater into a soil and establishment of threshold rainfall intensities. Pressure plate apparatus and method of continuous measurement with tensiometersare two techniques used for establishment of SWCC experimentally. It can also be derived from particle size distribution curves and plasticity limits using empirical correlations.Experimental processes are quite elaborate and time consuming. Hence comparison of SWCC obtained by the two approaches would be very helpful to gain confidence on the simpler empirical approach. The results of this research reveals that there a reasonably good agreement in the curves derived by the two approaches.

1 INTRODUCTION

Unsaturated soils consist of a four phase system with soil, water, air and air-water interface or contractile skin. (Fredlund and Rahardjo, 1993). The air-water interface (contractile skin) can exert a tensile pull and behaves as an elastic membrane which is under tension applied through the soil structure. This property can be identified as surface tension and results in an air pressure greater than the water pressure.

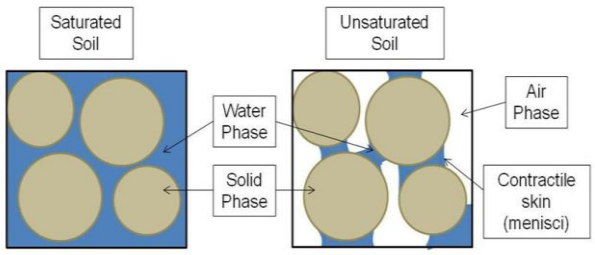

Figure 1: Four phases of an unsaturated soil

The difference in pore air and pore water pressures, i.e. matric suction, $u_a - u_w$ maintains water and air phases in equilibrium.

2 SOIL WATER CHARACTERISTIC CURVE

Soil Water Characteristic Curve (SWCC) represents the capacity of the soil matrix to hold moisture under varying matric suctions. It is defined as the relationship between volumetric water content and matric suction of the soil.

The volumetric water content, θ_w is defined as ratio between volume of water in the soil (V_w) to the total volume (V),$\theta_w = V_w/V$. When matric suction is increased during desorption, air-entry occurs and larger sized pores are initially drained.Figure 2 illustrates an idealized SWCC. Two important points in the curve are the air entry value and the residual water content.

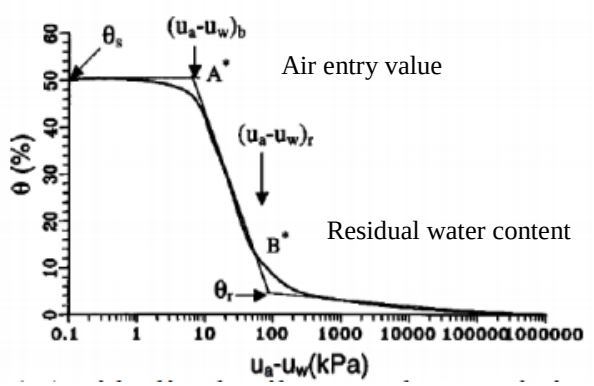

Figure 2: An idealized SWCC

Slopes in Sri Lanka are mainly made of residual soils and ground water table is generally low during dry periods. With high matric suctions prevailing in the soil above the ground water table slopes are quite safe. When rainfall infiltrates into the slopes, matric suctions are reduced or completely lost. Perched water table conditions may also develop with high intensity rainfalls. This will reduce the safety margins and may even lead to failure. Proper modelling of this process is essential in predicting the rain induced landslides.

SWCC and permeability function are the essential parameters in the process of modelling the infiltrationand should be established for all important slopes that are susceptible for failure.There are rigorous experimental procedures for this purpose. Also, researchers within last decade haveestablished methods for estimating the SWCC empirically using particle size distribution and plasticity limits, which is a much simpler approach. If the two approaches are tested and compared for soils forming Sri Lankan slopes it would create a confidence on the simpler approach and proper modelling of infiltration can be applied to many critical slopes. Vasanthan et al(2015) and Dilanthi et al (2018) have compared the SWCC obtained from a UD samples from the site of a failed slope and compacted Silty Clay used as a conventional fill material in Sri Lanka and compared with the Arya and Paris (1981) method.

3 ESTABLISHMENT OF BASIC CHARACTERISTICS OF SOIL SAMPLES

In this research comparison ofthe derived SWCC was done for two soil samples.One was a disturbed sample taken from a conventional fill material and the other was an undisturbed soil sample obtained from a cut slope in the Southern Expressway - Matara-Beliatta section. Disturbed sample was remolded by compacting at the optimum moisture content.

Initially, the basic soil properties were obtained for two soil samples. The Symbol for both soils under the Unified Soil Classification System was SM. The combined particle size distribution curves from Sieve analysis and Hydrometer analysis are presented in Figure 3.

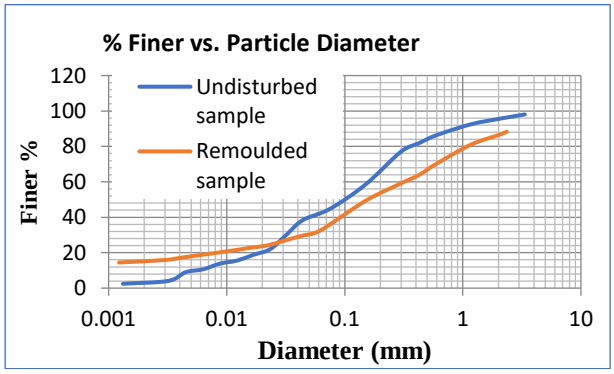

Figure 3: Combined particle size distribution curve for two soil samples

4 SWCC WITH PRESSURE PLATE APPARATUS

Pressure Plate Apparatus was one technique used for the experimental determination of SWCC.Figure 4 illustrates the major components of pressure plate apparatus. Soil samples were saturated and three specimens were extracted in to the PVC rings and kept inside the pressure plate apparatus on the high air entry disk. Then further water was added to ensure the saturation. After 24 hours, excess water was removed and air pressure necessary to obtain the expected matric suction was applied. The high air entry disc of capacity 500 kPa is saturated and open to the atmosphere which corresponds to a pressure of around 100 kPa. Thus the apparatus is capable of bringing the specimen to equilibrium under matric suctions up to 400 kPa.

The specimen was allowed to reach equilibrium under the applied air pressure. Equilibrium condition was confirmed when there is no flow of water out of the sample.Once the specimen reached the equilibrium, the weight was taken and saturated again. This procedure was continued increasingthe matric suctions from 20 kPa to 250 kPa.The volumetric water content at the equilibrium matric suction provided aredata points in the experimental curve.

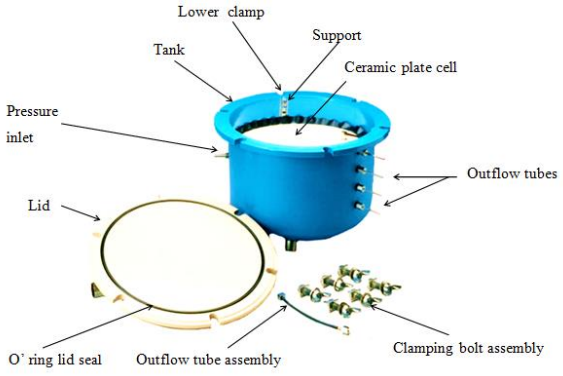

Figure 4: Major components of pressure plate apparatus

5 METHOD OF CONTINUOUS MEASUREMENT

In the method of continuous measurement a prepared saturated soil sample was allowed to dry or an unsaturated sample was wetted continuously while monitoring the change of matric suction. The volume of water flow is too small to measure and it was estimated by measurement of the weight of the sample. A miniature tensiometer developed by Jotisankasa et al (2010) at Department of Civil Engineering, Kasetsart University (KU), consisting of Micro Electro Mechanical 8 System (MEMs) pressure sensor, 1 BAR High-Air-Entry porous ceramic and transparent acrylic tube was used in this research to determine the permeability of the soil.

The sample (as compacted or undisturbed) was placed in the Perspex cylinder and the matric suction was measured continuously at three locations while recording the change of weight of

the soil sample. The tensiometers were connected to the sample at three locations as presented in Figure 5 and Figure 6.

Figur5: Tensiometer connected to the apparatus

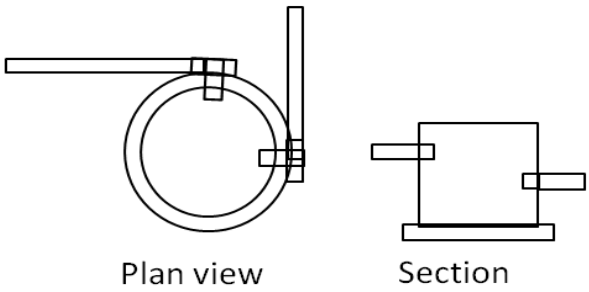

Figure 6: Plan view and the sectional view of the specimen

6 ESTABLISHMENT OF SWCC BY EMPIRICAL METHODS

6.1 Arya and Paris Method

Using the specific gravity, dry density and the particle size distribution of the soil, particle radii were converted in to a pore size distribution.

The accumulative pore volumes corresponding to progressively growing pore radii are divided by the sample dry density to give the volumetric water contents and the pore radii are converted to equivalent soil suctions using the equation of capillarity. The formulation is based on an empirical parameter, α, used to adjust the experimental results to the model. The variation of modal parameter with the particle diameterfor two soil types is presented in Figure 7.

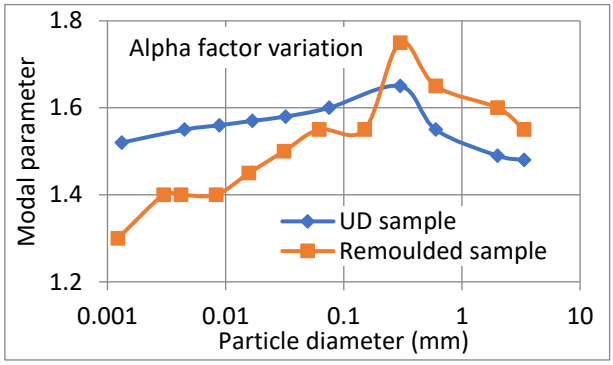

Figure 7: Variation of the modal parameter with particle diameter

6.2 Fredlund and Xing equations(1994)

Number of empirical relationships have been proposed by various researchers to predict the soil water characteristic curve using available soil data. Fredlund and Zing (1994) proposed a new equation to estimate the soil water characteristic curves of different soil contents of the soil at saturated and residual states and curve fitting parameters. These fitting parameters are determined based on the different interactions present between soil skeleton and the water phase.Fredlund and Xing equation (1994) is expressed as;

$$\theta(\psi,a,n,m)=C(\psi)\frac{\theta_s}{\left\{\ln\left[e+(\psi/a)^n\right]\right\}^m}$$

θ = Volumetric water content
ψ = Matric suction
θ_s = Saturated volumetric water content
a, n, m =Fitting parameters

Air entry value, rate of desaturation and residual water content were obtained according to the SWCC derived through experimental methods. The gravimetric water contents were converted to volumetric water contents, matric suction values were derived and the soil water characteristic curves were obtained as a continuous function.

6.3 Zapata model(1999)

Zapata (1999) proposed a model to estimate the soil water characteristic curve, based on the soil index properties and fitting parameters used in the equation proposed by Fredlund and

Xing (1994). The model separately accounts for both plastic and non-plastic soils. Correlations between the index properties and fitting parameters have been derived based on available soil data. Atterberg Limits, percentage passing No: 200 sieve and D_{60} from the particle size distribution curve, are used in derive fitting parameters to predict SWCC.

The proposed equation is;

$$\Theta_w = C(h) \times \left[\frac{\Theta s}{\left[ln\left[exp(1) + \left[\frac{h}{a} \right]^b \right] \right]^c} \right]$$

a : A soil parameter which is a function of the air entry value of the soil in kPa

b : A soil parameter which is a function of the rate of water extraction of the soil, once the air entry value has been exceeded

h : A soil parameter which is function of residual water content in kPa.

C(h): An adjustment function to direct all the curves to zero water content at the suction of 1,000,000 kPa

Zapata (1999) introduced correlations to determine the above fitting parameters using the basic soil properties.

7 COMPARISON OF THE RESULTS

SWCCs obtained for undisturbed soil sample and the remoulded soil sample by the different techniques are presented in Figure 8 and Figure 9.

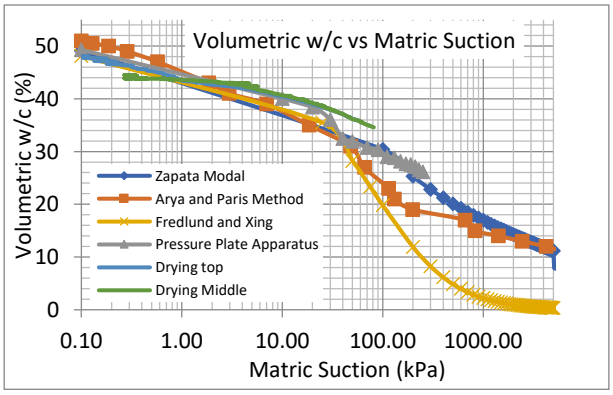

Figure 8: SWCC for remoulded soil sample

According to figure 8 and figure 9, SWCCs obtained through both experimental and numerical methods are consistent within the range of experimental results.

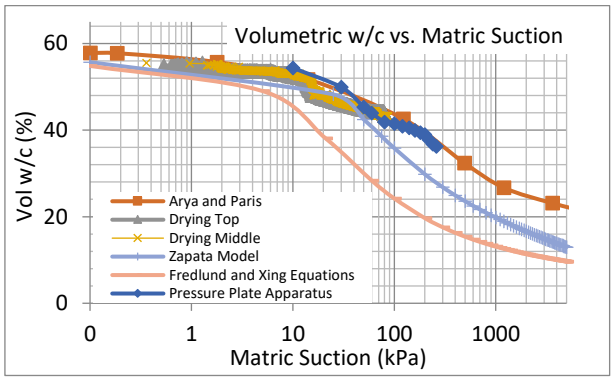

Figure 9: SWCC for undisturbed soil sample

Results obtained from wetting method seems to be much deviated from realistic values.This might be due to irregular infiltration of water and accumulation of water on the surface. Hence the wetting path results are removed in the comparison.

8 CONCLUSION

For lower matric suction ranges (<100 kPa), proposed models could be used to predict SWCC with a higher degree of accuracy.The empirical correlations can be extended up to higher matric suction values. But the accuracy of those results has to be examined using experimental methods.When matric suction exceeds 250 kPaFredlund and Xing results are much deviated from other empirical results as the higher slopes of the curves.

9 REFERENCES

Arya, L.M. & Paris, J.F., (1981), “A physic-empirical model to predict the soil moisture characteristic from particle size distribution and bulk density data”, Soil Sci. Soc. Am. J. 45: pp. 1023–1030..

Jotisankasa, A., Tapparnich, J., Booncharoenpanich, P., Hunsachainan, N. andSoralump, S., (2010), “Unsaturated soil testing for slope studies”, Proc. International conference on Slope, Thailand 2010, Geo-technique and Geo-synthetics for Slope, Chiangmai, Thailand.

Fredlund, D. G. and Rahardjo, H.,(1993), “Soil mechanics for unsaturated soils”. New York: Wiley.

Dilanthi H P W, Kulathilaka S A S and Vasanthan N, Shear strength and Permeability Characteristics of some Sri Lankan Residual soils, Paper published at the UNSAT2018 conference held in Hong Kong 2018

Fredlund, D.G., Anquing Xing and Shangyan Huang, (1994) “Predicting the permeability function for unsaturated soils using soil water characteristic curve”, Canadian Geotechnical Journal, volume 31(3): pp. 521-532.

Vasanthan, N., Kulathilaka, S.A.S., Properties of an Unsaturated Residual Soil behind a Failed Slope in Sri Lanka, Paper acceptedfor publication in the Journal of the SouthEast Asian Geotechnical Society, 2019

Zapata, C., Houston, W.N., Houston, S. and Walsh, K.D., 2000. Soil-water characteristic curve variability. In The GeoDenver 2000-Unsaturated Soils Sessions' Advances in Ultrasound Geotechnical' (pp. 84-124). ASCE.

Correlations among Index Properties, Strength and Compressibility Parameters of Some Sri Lankan Peat Soil

T. Chenthan, S. Sharuja, M.C.M. Nasvi
Department of Civil Engineering, University of Peradeniya, Sri Lanka

ABSTRACT: Peat is an extreme form of soft soil and its geotechnical properties cannot be determined so easily as it is water logged most of the time. Developing of correlations among different properties of peat will enable to study the geotechnical properties of peat. Hence, aim of this paper was to develop a correlation among index properties, uniaxial compressive strength (UCS) and compressibility parameters of some Sri Lankan peat soils. Fifteen disturbed and undisturbed samples were collected in Muthurajawela region, Sri Lanka and index properties tests, UCS test and 1-D consolidation tests were conducted for all the samples. Seven correlations were developed based on the experimental results and it was noted that the correlations developed were consistent with similar correlations reported in the literature. The results show that the LL of peat increases with the increase in both OC and WC. In addition, both the G_S and UCS values reduce with the increase in OC value. When the WC content increases, the UCS of peat tends to reduce as the water holding capacity of peat increase with the increase in WC. The C_C value reduces with the increase in LL and it is due to the increase in compressibility with the increase in LL. Findings of this study revealed that geotechnical engineers can refer these correlations to study the preliminary behavior of Sri Lankan peat soil, where the geotechnical data are not readily available.

1 INTRODUCTION

Peat is a soft soil made up of partially disintegrated plant and organic matters that have accumulated under water and fossilized(Moore, 1989). The decaying process of plant under acidic condition without microbial process results in the formation of organic matter in peat (Sing, et al., 2008). Characteristics of peat are low bearing capacity, low specific gravity, medium to low permeability, high compressibility, high natural water content, high water holding capacity, high rates of creep and difficult accessibility(Kolay, et al., 2010, Dehghanbanadaki, et al., 2013). According to Bord and Mona (1984), peat lands covers nearly 400 million hectares of the earth which is 3% of the total land surface area. In Sri Lanka, there are 25000 hectares of peat land (Venuja, et al., 2017). Peat is classified into two major types such as fibrous and amorphous. Von Post (1922)further divided this into ten different ranges using Von Post scale system. In this system, peat is divided from H1 (completely fibrous peat) to H10 (completely amorphous peat) based on degree of humification, water content, fiber content and botanical composition (Huat, et al., 2010). According to ASTM Standard D4427, standard peat classification is narrowed to three classes namely fibric (fibrous; least decomposed with fiber content of more than 67%), hemic (semi-fibrous; intermediate decomposed) and sapric (amorphous; most decomposed with fiber content of less than 33%). As these are extremely soft soils, it is very difficult to determine its physical and geotechnical properties (Kolay, et al., 2010). It is convenient to relate the basic geotechnical properties of peat with few of the easily determined index or physical properties of peat. Hence, development of correlation between different properties will be useful.

However, to date there are very limited studies focusing on the correlation between different properties of Sri Lankan peat soil. Hence, aim of this research was to develop a correlation among index properties, strength and compressibility parameters of Sri Lankan peat soil. The detailed experimental methodology and the results are discussed in the following sections.

2 MATERIALS AND METHODS

2.1 *Materials*

Peat samples for our experimental analysis were collected from two different locations on the both side of Colombo - Katunayake expressway (CKE) located in the western province of Sri Lanka. Figure 1 describes the location of the sampling.

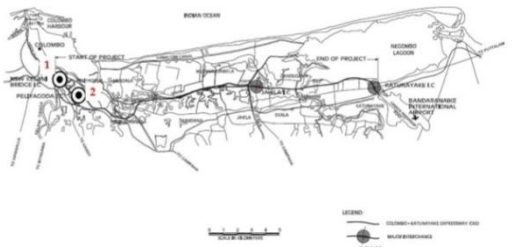

Figure 1: Location1 (L1) and Location 2 (L2) of Sample Collection.

From locations 1 and 2, fifteen undisturbed samples were collected using PVC tubes of 150 mm diameter and 400 mm height. One end of the PVC tube was taped to sharpen the edges to facilitate the drilling. Undisturbed samples were waxed immediately after the extraction from the field mainly to avoid the loss moisture content of the samples. From each sample locations, disturbed samples also were collected for the index properties test.

2.2 *Experimental procedure*

Index properties tests including moisture content (BS 1377: part 2: 1990), atterberg limits (BS 1377: Part 2: 1990), loss on Ignition (BS 1377: part 3: 1990) andspecific gravity (BS 1377: part 2: 1990) were conducted. Further, uniaxial compression test (BS 1377: part 7: 1990) and 1-D Consolidation test (BS 1377: part 5: 1990) were also conducted for all the peat samples.

Based on the experimental outcomes the following correlations were developed: Liquid Limit (LL) vs Organic content (OC); Liquid Limit (LL) vs Water content (WC); Organic content (OC) vs Water content (WC); Specific gravity (G_S) vs Organic content (OC); Uniaxial Compressive Strength (UCS) vs Liquid limit (LL); Uniaxial Compressive Strength (UCS) vs Organic content; Compression index (C_C) vs Liquid Limit (LL).

3 RESULTS AND DISCUSSION

The overall experimental results indicated that the index properties such as natural water content, liquid limit, organic content and specific gravity ranged from 12.2-164.8 %, 41.6-96.2 %, 4.3-32.9 % and 1.73-2.59 respectively, Uniaxial compressive strength values of these peats vary from 9.2-49.8 kPa and the compression index varies from 0.15-1.875.

Figure 2 shows the plot of liquid limit with organic content and similar plots from the literature. The obtained relationship between LL and OC is given in Equation (1).

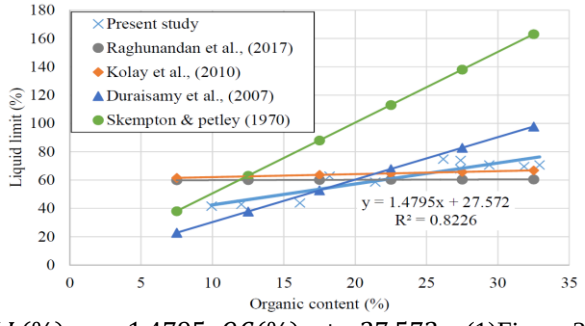

$$LL(\%) = 1.4795\ OC(\%) + 27.572 \quad (1)$$

Figure 2: LL (%) vs OC (%)

The results shows that *LL* increase with *OC*. It is widely accepted that the available water holding capacity of soil increases with the increase in organic matter content. Along with the increase in *OC*, the water holding capacity of the peat soil become higher leading to increase in the *LL* values (Huat, et al., 2009,Duraisamy, et al., 2007).

LL increases with WC as shown in Figure 3 and the developed correlations is given in Equation (2).

$$LL(\%) = 13.703\ ln(WC(\%)) - 2.7103 \quad (2)$$

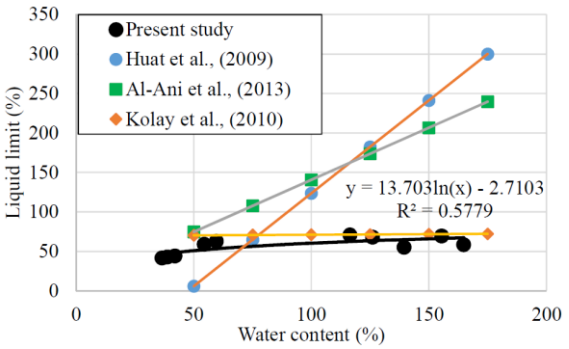

Figure 3: LL(%) vs WC(%)

Higher natural water content interprets the higher water holding capacity of peat soil. Higher water holding capacity leads the peat soil to higher *LL*. The *LL* values of Sri Lankan peats are less sensitive to change in *WC* compared to the peat reported in the literature.

Figure 4 shows the relationship between organic content and water content and the developed correlation between OC and WC is given in Equation (3).

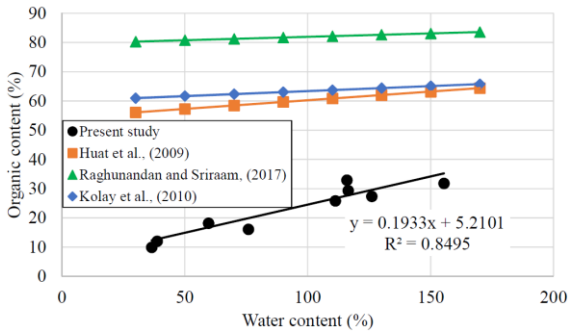

$$OC(\%) = 0.1933\ WC(\%) + 5.2101 \quad (3)$$

Figure 4: OC (%) vs WC (%)

Increase in *OC* in peat soil increases the water holding capacity of peat soil. Because of the higher *OC*, the natural *WC* of peat also increases(Kolay, et al., 2010, Huat, et al., 2009). Sri Lankan peat shows lower *OC* values compared to the peat reported in the literature (Figure 4).

Figure 5 shows the relationship between specific gravity with organic content and the developed correlation between specific gravity and organic content is given in Equation (4).

$$G_S = -0.032\ OC(\%) + 2.8846 \quad (4)$$

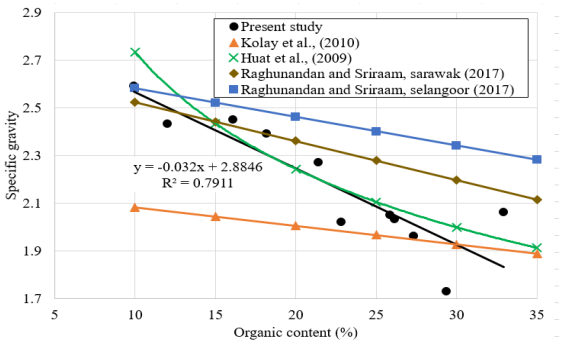

Figure 5: G_S vs OC(%)

As high *OC* implies more air voids, the increase in *OC* greatly affect the G_s of peat soil. Therefore, G_s reduces with the increase in *OC*. It can be seen that Muthurajawela peat is more sensitive to the *OC* variation compared to the peats reported in the literature(Raghunandan & Sriraam, 2017, Kolay, et al., 2010, Huat, et al., 2009).

The relationship between the Uniaxial Compressive Strength and liquid limit is shown in Figure 6 and the developed correlation is given in Equation (5).

$$UCS(kPa) = -0.6256\ LL(\%) + 67.779 \quad (5)$$

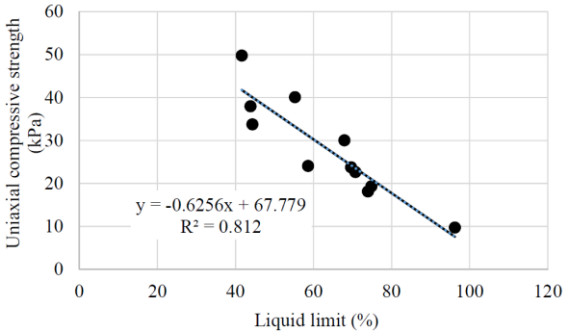

Figure 6: UCS (kPa) vs LL (%)

According to Figure 8, increase in *LL* results in reduction in UCS value and it is because the rises in *LL* increase the water holding capacity. As the water content increases, effective stress reduces leading to reduced *UCS* values.

The relationship between uniaxial compressive strength and organic content is shown in Figure 7 and the developed equation is given in Equation (6).

$$UCS(kPa) = -1.1951\ OC(\%) + 55.973 \quad (6)$$

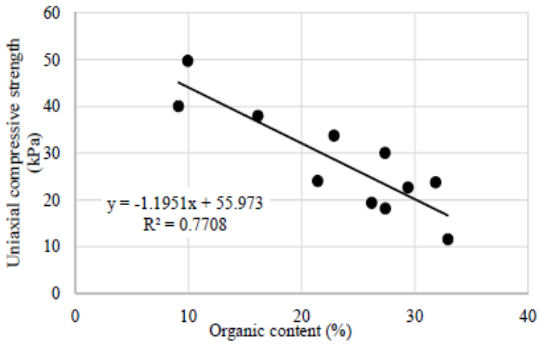

Figure 7: UCS (kPa) vs OC (%)

The result shows that *UCS* decreases with increasing *OC*. Increase in *OC* in peat soil increases the water holding capacity of the peat soil leading to increase in *WC*. The *UCS* of peat reduces as the WC increases.

Figure 8 shows the relationship between compression index and liquid limit and it can been seen that the developed plot well matches with the existing literature. The developed correlation is given in Equation 7.

$$C_C = 0.0117\ LL(\%) - 0.244 \quad (7)$$

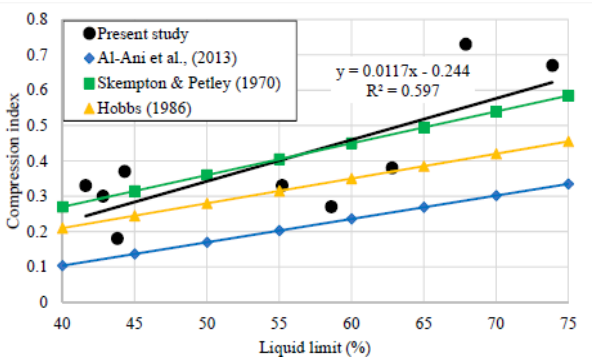

Figure 8: CC vs LL (%)

As the *LL* increases, water holding capacity of peat increases. Higher water holding capacity leads to higher compression leading to increase in C_c values.

The applications of the above correlations are as follows:

1. Estimation of complex geotechnical parameters (UCS, CC) using few simple index properties (WC, LL, OC, G_S) of peat.
2. Quick estimation of primary consolidation settlements by knowing simple index properties.
3. Proposing ground improvement techniques by identifying compressibility parameters through these correlations.

4 CONCLUSIONS

Based on the experimental results, the following correlations were developed;

1. LL (%) = 1.4795 OC (%) + 27.572
2. LL (%) = 13.703 ln(WC (%)) − 2.7103
3. OC (%) = 0.1933 WC (%) + 5.2101
4. GS = −0.032 OC(%) + 2.8846
5. UCS (kPa) = −0.6256 LL (%) + 67.779
6. UCS (kPa) = −1.1951 OC (%) + 55.973
7. CC = 0.0117 LL (%) − 0.244

These correlations can be used to determine complex geotechnical parameters of peat by knowing easily determine simple index properties and to propose suitable ground improvement techniques of peat.

REFERENCES

Bord na Mona, 1984. *Fuel peat in developping contries,* Dublin: World bank.

Dehghanbanadaki, A., Ahmad, K. & Ali, N., 2013. Influence of natural fillers on shear strength of cement treated peat. *GRADEVINER,* 65(7), pp. 633-640.

Duraisamy, Y., Aziz, A. A. & Huat, B. B. K., 2007. Engineering Properties and Compressibility Behavior of Tropical Peat Soil. *American Journal of Applied Sciences,* 4(10), pp. 768-773.

Huat, B. B., Asadi, A. & Kazemian, S., 2009. Experimental Investigation onGeomechanical Properties of Tropical Organic Soils and Peat. *American J. of Engineering and Applied Sciences* , 2(1), pp. 184-188.

Huat, B. B. et al., 2010. Influence of cement-sodium silicate grout admixed with calcium chloride and kaolinite on sapric peat. *Journal of civil engineering and management,* Volume 17, pp. 309-318.

Kolay, P. K., Aminur, M. R., Taib, S. N. L. & Zain, M. I. S. M., 2010. Correlation between Different Physical and Engineering Properties of Tropical Peat Soils from Sarawak. *Soil Behavior and Geo-Micromechanics.*

Moore, P. D., 1989. The ecology of peat forming processes. *International Journal of Coal Geology,* 12(1-4), pp. 89-103.

Raghunandan, M. E. & Sriraam, A. S., 2017. An overview of the basic engineering properties of Malaysian peats. *Geoderma Regional,* Volume 11, pp. 1-7.

Sing, W. L., Hashim, R. & Ali, F. H., 2008. Behaviour of stabilized peat soils in unconfined compression tests. *American J. of Engineering and Applied Sciences,* 1(4), pp. 274-279..

Venuja, S., Mathiluxsan, S. & Nasvi, M. C. M., 2017. Geotechnical Engineering Properties of Peat, Stablized with a Combination of Fly Ash and Well Graded sand.. *Journal of the Institution of Engineers, Sri Lanka,* 50(2).

von Post, L., 1922. Sweden's Geological Survey's Tournament and some of its achievements so far.. *Swedish Museum of Mammals Association (0371-4446),* Volume 37, pp. 1-27.

Comparison of Triaxial Mechanical Behaviour of Geopolymer and OPC under Downhole Conditions

T. Panchalingam, K. Sinthulan and M. C. M Nasvi
Department of Civil Engineering, University of Peradeniya, Sri Lanka

ABSTRACT: Carbon capturing and storage (CCS) is found to be the best solution to reduce anthropogenic greenhouse gas from the atmosphere. To date, ordinary Portland cement (OPC) based cement has been used in the sequestration wells and it has been found that it cannot sustain as well cement for long term. Instead, geopolymer can be good alternative for OPC as it has high strength and excellent resistant characteristics. A typical well cement is exposed to various temperatures, confining stresses and salinity depending on the geological location and depth. Therefore, aim of this research was to study the triaxial mechanical behavior of geopolymer and OPC under different salinity and confining stresses. This research comprised of experimental and numerical works. Under the experimental work, series of uniaxial compressive strength (UCS) test were conducted for geopolymer and OPC samples cured at 0 – 30% NaCl salinity for 45 days. COMSOL Multiphysics FEM package was used for the numerical study, the lab scale stress-strain behaviour of geopolymer and OPC was validated. The model was then extended to study the triaxial behaviour under different salinity (0-30% NaCl) and confinements (0-15 MPa). Based on the results, it was noticed that UCS of geopolymer increases with salinity whereas it reduces for OPC towards high salinity. In addition, failure strength of geopolymer significantly increases with increase in both salinity and confining stress and the values were significantly higher compared to OPC. On the whole, it is concluded that geopolymers can be a good alternative to OPC as a well sealant material.

1 INTRODUCTION

The global warming is increasing day by day mainly due to the increased emission of carbon dioxide. In order to reduce theCO_2 concentration in the atmosphere, carbon capture and storage (CCS) is preferred to other mitigation measures in terms of efficiency and effectiveness. The success of CCS process depends on the behaviour of the well cement under down-hole conditions. To date, OPC based well cement is used in these wells and it has been found that it degrades under downhole environment On the other hand, it has been found that geopolymer possesses higher strength, better durability and excellent acid resistance characteristics A typical well bore experiences different temperatures with a geothermal gradient of 30 °C/km, different salinity (0-30% NaCl) and different confinements. Therefore, major aim of this research was to study the triaxial mechanical behaviour of geopolymer and OPC under different downhole conditions.

Many researches have been done in the area of well cement by considering the factors such as different salinity levels, temperature, water-cement ratios and etc. Pan et al (2009) investigated the mechanical behaviour of geopolymer exposed to elevated temperatures. It was found that, at the elevated temperatures, geopolymer samples showed a strength variation and it is governed by two processes: sintering or geo polymerization and thermal incompatibility. Strength gain or loss is based on the dominant factor among those two factors.

Lecolier et al (2007) studied the durability of hardened Portland cement paste used in for the oil well cementing. The compressive strength of hardened cement paste aged in brine water with monthly renewal was reduced with time. This degradation was due to the leaching of portlandite and the appearance of micro cracks due to depressurization.

2 METHODOLOGY

2.1 Experimental work

Geopolymer was prepared using fly ash as the source material and it was obtained from Norochcholai power plant, Sri Lanka. Geopolymer paste was prepared with a fly ash to alkali liquid ratio of 0.6 and OPC paste waste was prepared with a water to cement ratio equals to 0.44. Cylindrical samples of 38 mm diameter and 76 mm height were casted and heat cured at 50° C for 24 hours as shown in Fig. 1 below. Immediately after

heat curing, three samples from each type were tested and the control strength values were obtained. Remaining samples were cured in 0% to 30%NaCl salinity saline medium for 45 days. Uniaxial compressive strength (UCS) test was conducted for all the samples.

Fig. 1Heat cured samples

2.2 Numerical work

COMSOL Multiphysics was used to study the triaxial mechanical behaviour of these well cements (geopolymer and OPC) under higher confining stresses, as the existing triaxial setup cannot fail cement samples with high confining stresses. Thenumerical analysiswas initiated with model validation and followed with the model extension.

Under the model validation, laboratory based UCS behaviour was simulated in COMSOL and the results were compared with laboratory stress-strain results to validate the numerical model. The boundary conditions were applied according to Fig. 2 and the modelled mesh shown in Fig. 3 was developed.

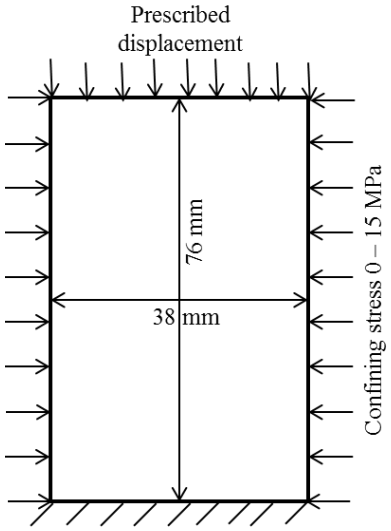

Fig. 2Boundary condition used for the FEM analysis

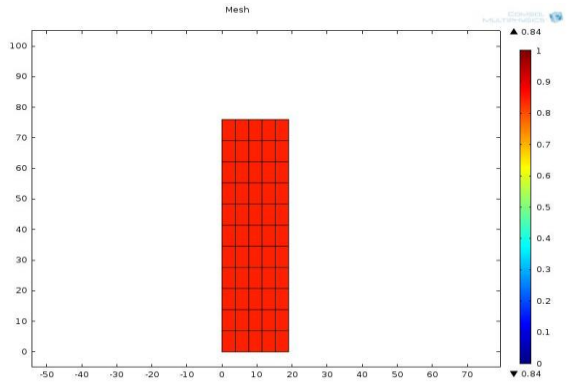

Fig. 3FEM mesh used in the modelling

In the model extension, validated model was extended by applying confining stresses of 0, 5, 10 and 15 MPa. In the solid mechanics module the linear elastic material was selected for concrete and initial stress- strain condition was provided. The failure stress was calculated by integrating the z component of the stress using equation (1).

$$Fres = \int \sigma z . 2\pi r dr \quad (1)$$

WhereF_{res} is the resultant force, $\sigma_z$is the z component of the stress tensor at each Gauss point and r is the radius of the geometry in cylindrical coordinates.Table 1 shows the model parameters used for the modelling.

Table 1: Model parameters and values

Model Parameters	Values
Uniaxial tensile strength	10% of UCS
Biaxial compressive strength (BCS)	116% of UCS
Poission's ratio	0.26
Prescribed displacement	0.05 to 1 mm
Confining stresses	0 to 15 MPa

3 RESULTS AND DISCUSSION

3.1Experimental results

Fig. 4 shows the variation of Uniaxial compressive strength (UCS) for geopolymer and OPC with different salinity levels. The UCS results of geopolymer increases with salinity as the salt content acts against weakening of samples. When compared to control samples, strength of geopolymer reduces due to the alkali leaching initiated with ageing. Based on Giasudeen et al(2013) findings, it was noticed that the rate of strength reduction is reducing with salt content

Whereas compressive strength of 45 days cured samples is higher than that of control OPC samples as the hydration process causes the strength increment. Strength of OPC samples increases as the NaCl concentration is increased up to 10% salinity

level because of the initial absorption of NaCl micro crystallites. But, it reduces at high salinity levels as the high salt content retards the hydration process and strength gain process. Gowthaman et al(2016) results showed similar behaviour.

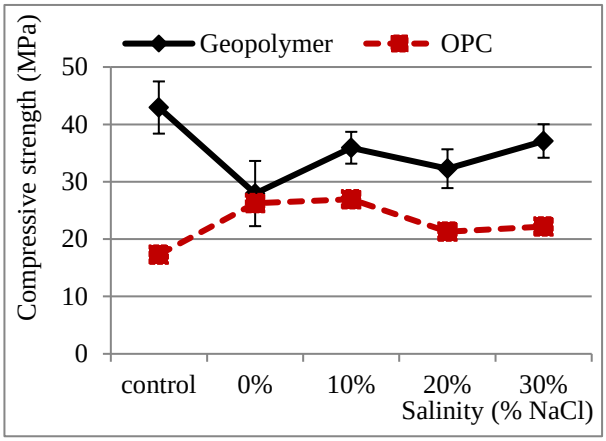

Fig. 4Variation of UCS for geopolymer and OPC with different salinity levels.

Fig. 5 illustrates the Young's modulus variation with salinity for both geopolymer and OPC. Young's modulus of geopolymer initially increases because of the absorption of NaCl micro crystallites. But, it reduces towards high salt content as the salt content reduces the stiffness. Stiffness of OPC also follows similar trend as its UCS. However the geopolymer possesses high Young's modulus values in all the salinity levels.

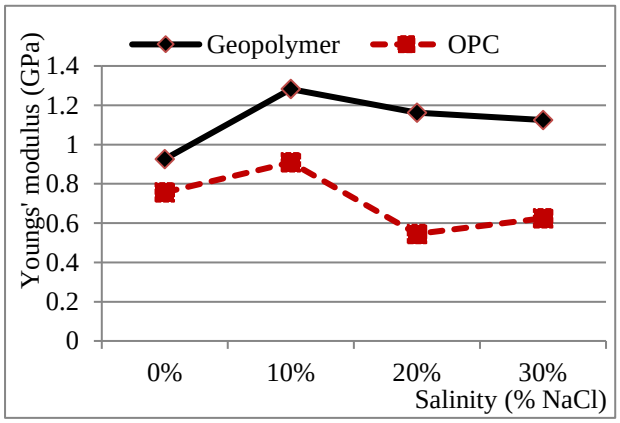

Fig. 5Variation of Young's Modulus for geopolymer and OPC with different salinity levels.

3.2 Numerical results

Fig. 6 compares the stress-strain plot obtained for geopolymer from the experimental and COMSOL simulation. Predicted stress-strain results are consistent with the experimental findings for both geopolymer and OPC samples. According toNasvi etal (2015),it was not possible to obtain the full plastic region of the stress-strain plot from the experiment, as these materials are brittle. Model predicts the behaviour well up to yield point and it assumes perfectly plastic behaviour after the yield point.

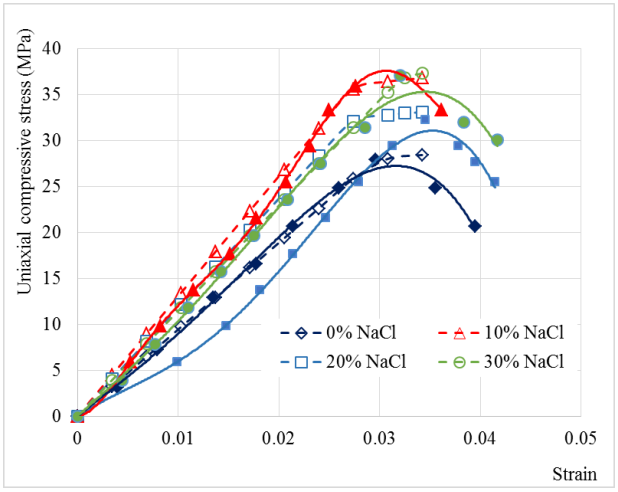

Fig. 6: Experimental and modelled stress-strain curve for geopolymer (Solid bullet points- Experimental and Hollow bullet points- Numerical)

Figs. 7 and 8present the results of the failure strength variation with salinity for the geopolymer and OPC samples respectively.

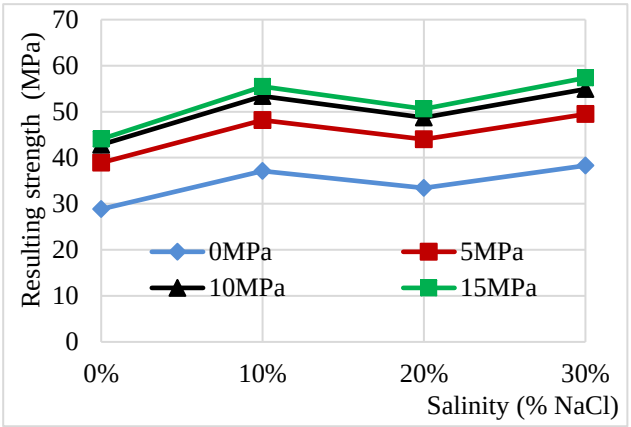

Fig 7: Variation of Resulting strength of geopolymer with salinity.

Pore voids in the geopolymer samples reduce its mechanical strength. Failure stress of both samples increases as the confining stress is increased because the applied confining stresses makes the pore voids become closer and increase the mechanical strength. The results were further supported by Nasvi et al (2015). Failure strength of geopolymer increases with salinity as it acts against alkali leaching as shown in Fig. 7.

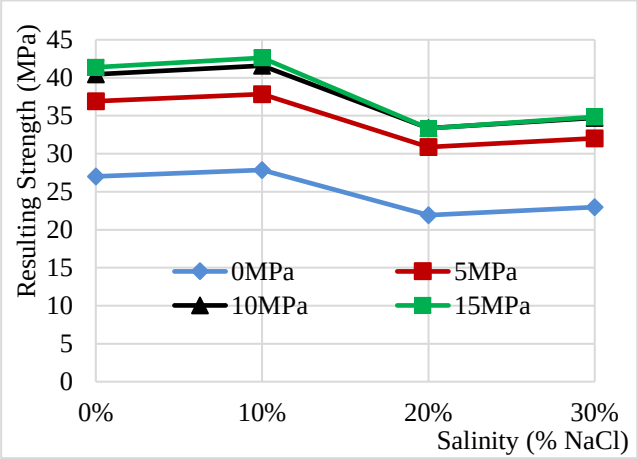

Fig. 8: Variation of Resulting strength of OPC with salinity.

On the other hand, failure stress of OPC increases up to 10% NaCl and reduces at high salinity levels. The effect can be illustrated as, the NaCl microcrystal absorption was high at the favourable10% salinity level. When the salinity further increases, the samples were degraded and results in failure strength reduction.

4 CONCLUSIONS

Based on the findings of this research, following conclusions were drawn:

- Compressive strength of geopolymer increases with NaCl concentration due to the resistance against alkali leaching.
- The UCS of OPC increases up to 10% NaCl, due to the absorption of NaCl micro crystallites and beyond that it reduces. High salt content degrades the samples and retards the hydration process.
- Predicted stress- strain results were consistent with the experimental findings up to yield point.
- Resulting stress increases with increasing confinement for both geopolymer and OPC as the confining stress reduces the pore void ratio which results in stress increment.
- On the whole, geopolymer can replace OPC in well cementing application because of its higher mechanical strength and improved plastic properties.

ACKNOWLEDGMENTS

The authors of this work were supported by the Faculty of Engineering, University of Peradeniya.

REFERENCES

Barlet-Goue´dard V , Rimmele G , Porcherie O , Quisel N , Desroches J. (2009). A solution against well cement degradation under CO2 geological storage environment, International Journal of Greenhouse Gas Control,3: 206 – 216.

Giasuddin M.H, Sanjayan J, Ranjith P.G (2013),Strength of geopolymer cured in saline water cured in ambient conditions, FUEL

Gowthaman S, Krishnya S, Nasvi M C M(2016), Effect of salinity on mechanical behaviour of well cement: Application to carbon capture and storage wells, Engineer-Vol. XLIX, No. 01, pp.[21-29]

Lecolier E, RivereauA, Saout GL, Audibert HA. (2007). Durability of Hardened Portland Cement Paste used for Oilwell Cementing, Oil & Gas Science and Technology Vol. 62 (3): 335-345.

Nasvi M C M, Ranjith P G, Sanjayan J (2015). A numerical study of triaxial mechanical behaviour of geopolymer at different curing temperatures: An application for geological sequestration wells, Journal of Natural Gas science and Engineering 26 (2015) 1148-1160

Pan Z, Sanjayan J G Rangan B V(2009), An investigation of the mechanisms for strength gain or loss of geopolymer mortar after exposure to elevated temperatures, J Mater Sci 44 : 1873-1880

Investigation of Strength Behavior in Soft Peaty Clays Stabilized with Calcium Carbide Residues and Fly Ash

T.H. Vitharana, A.S. Ranathunga
Department of Civil Engineering, University of Moratuwa, Sri Lanka

ABSTRACT: Presence of underground thick peaty clay layers is a serious issue for the Sri Lankan construction industry. Due to the high compressibility and the low shear strength of the peaty clay, necessary improvements for the soil shall be done prior to the construction. Deep mixing of soil with cement gives the adequate strength in a short period of time however not effective in cost. This study is about the usage of industrial by-products like Calcium carbide residue (CCR) and Fly ash (FA) for the stabilization of peaty clay during deep mixing method. Unconsolidated undrained shear strength parameters of the samples were determined and in order to understand the microstructural changes of the treated soil specimens, a microstructural study using the scanning electron microscope (SEM) is performed.The results show that the strength improvement of peaty clay with CCR content occurs in three zones: active, inert and deterioration. Further, adding FA will be much effective in the deterioration zone.

1 INTRODUCTION

Rapid development in the construction industry leads the geotechnical engineers to emphasize on the improvement of weak soil. Since the demand for the land is getting high, the industry has to look for new lands that have no favorable conditions for constructions which have underlaying peaty clay.

The peaty clays which is frequently encountered in the highway embankments in Sri Lanka are with a water content of nearly or more than 300% and have a shear strength as low as 2kN/m^2 (Madushanka, 2015). Peat consists of organic and fiber matter and the classification of peat is based on degree of humification (von post scale). Presence of the organic matter in peat clay is a critical issue since further decomposition of this organic matter due to the environmental changes leads to the utter failures of the structures made on peaty lands. Peat has the ability to take up of water and hold it. Due to the high-water amount, high pore volume (high void ratio) is present and therefore it has low bulk density and low bearing capacity. Further lowering the ground water table may cause the shrinkage of peaty clay.

Although the shear strength of peaty clay is very low it can be made high by consolidation. However, the primary and secondary consolidation processes are time dependent. Primary consolidation is due to the dissipation of excess pore water pressure caused by the increase in effective stress followed by the secondary consolidation where the compression of fibrous peat occurs under constant effective stress. Permeability plays a major role in consolidation since it speeds up the process. Previous studies reveal that the peat is averagely porous and therefore has a medium state of permeability (Kolay and Pui, 2010).

Various techniques have been adopted to improve the strength characteristics of peaty clay. Preloading is a technique where soil undergoes primary and secondary consolidation. The embankments are preloaded with a surcharge greater than the load expected on the embankment during the operational stage. Construction of the embankment is done in stages and much time is allocated for the consolidation in each stage which is not time and cost effective for a project.Replacing the weak soil with granular soil is another practice that can be adopted however absence of a proper way of disposal of the peaty clay to the environment is a problem.

1.1 *Cement as a stabilizer*

Deep mixing method is currently being practiced in the world as a ground improvement technique. The soft soil is mixed in-situ with different binders which will give early strength compared to preloading method. The hydration reaction occurs when cement is used as the binder is shown in Eq. (1).

$$\text{Cement} + \text{water} \rightarrow \text{CSH} + \text{CAH} + \text{CASH} + \text{Ca(OH)}_2 \quad (1)$$

In the cement hydration process hydrated calcium silicates (CSH), hydrated calcium aluminates (CAH),hydrated calcium aluminum silicates (CASH), hydrated lime [Ca(OH)$_2$] are the main products(formation of primary cementitious mate-

rials). There is an increase in pH value of the medium due to the dissociation of $Ca(OH)_2$ which let the silica and alumina from the soil to be dissolved as an acid dissolves in a strong base. The hydrous silica and hydrous alumina then gradually react with Ca^{2+} ions to form secondary cementitious materials. Formation of cementitious materials which get hardened with time and dissipation of pore water for the hydration process make the peaty clay to be stabilized rapidly(Horpibulsuk et al., 2011).

Madhusanka(2015) reveals that the ratio of 20-25% of cement is generally used with soil in order to have a considerable improvement in peaty clay. It is about 250kg needed to stabilize $1m^3$ of embankment which is both economically and environmentally (CO_2 emission due to cement manufacturing) unfeasible.

1.2 *Calcium carbide residue and Fly ash*

The aim of this research is to find the alternatives for cement to be used in the industry as stabilizers of peaty clay. An attempt is made to investigate the possibility of using Fly Ash (FA) and Calcium Carbide Residue (CCR) to improve the strength characteristics of the peaty clay which is taken from Southern Expressway extension.

Fly ash is a waste product of thermal power plants and Norochcholai coal power plant in Sri Lanka which generates FA around 150MT per year (Venuja et al., 2017). There are two types of Fly ash as Class F and Class C. Class C FA normally comes from coals which contains high lime content than Class F FA. The percentage by weight of SiO_2, Al_2O_3 and Fe_2O_3 is greater than 70% in class F Fly Ash and in the range of 50-70% in class C Fly Ash. Compared to Class C FA, Class F has lesser Ca compounds which reduces the ability for proper pozzolanic reaction (Nalbantoğlu, 2004). In Norochcholai power plant, it generates Class F FA and hence is needed to add a high Ca additive to accelerate the pozzolanic reaction. One such additive is CCR.

CCR is a by-product of acetylene gas factories and it is a waste product in the industry derived as shown in Eq. (2)

$$CaC_2 + 2H_2O \rightarrow C_2H_2 + Ca(OH)_2 \quad (2)$$

$Ca(OH)_2$ is disposed in slurry form and after being sun dried it becomes dry form which is known as CCR. 64 g of calcium carbide (CaC_2) provides 26 g of Acetylene gas (C_2H_2) and 74 g of CCR, in terms of $Ca(OH)_2$ that is an abundance as a raw material (Horpibulsuk et al., 2012). There is a demand increasing for a way of disposal of CCR since it is very difficult to dispose to the nature being a highly basic material.

2 METHODOLOGY

Peaty clay sample was obtained from the Southern Expressway extension at Beliaththa. Debris were removed and a homogeneous sample was prepared. Basic Engineering properties of the soil sample were determined and shown in Table 1.

Table 1. Basic properties of peaty clay

Basic Property	Value
Moisture Content (%)	400
Bulk Density (kN/m^3)	10.83
Specific Gravity (Gs)	1.819
pH Value	2.3
Organic Content (%)	40.5
Fibre Content (%)	24
Liquid Limit (%)	62
Initial Void Ratio	4.303

Peat was mixed with cement, CCR and FA according to different mix proportions by weight (Table2). The mixing percentages are the percentage weight of each additives out of the weight of the peaty clay used for the sample. Mixing was done with an aid of a mechanical mixer (Fig. 1). Prepared samples were kept in buckets and a surcharge of $10kN/m^2$ was applied for 28 days and 90 days separately for shortterm and longterm stabilization respectively (Fig. 2). Since the moisture in the peat is dissipated for the hydration process water was put in to the buckets at regular time periods.

Table 2. Mix proportions

Combination	Mix proportion
Peat only	Peat 100%
Peat + Cement	Cement 20%
Peat + CCR	CCR 10% , CCR 15%, CCR 20%
Peat + CCR +FA	CCR 10% + FA 10%
	CCR 10% + FA 20%
	CCR 15% + FA 10%
	CCR 15% + FA 20%
	CCR 20% + FA 10%
	CCR 20% + FA 20%

A sampler was inserted into the bucket, samples were taken and extruded in to a mould. Unconsolidated undrained tri axial tests according to ASTM D2850 were carried out for three samples of each mix proportion having three different cell pressures $50kN/m^2$, $100kN/m^2$ and $150kN/m^2$ (Fig. 3). Engineering properties of the samples of each mix proportion were determined for short term and long term.

Fig. 1 Mechanical mixer

Fig. 2 Loading Mechanism

Fig. 3 Tri-axial Testing

3 RESULTS AND DISCUSSION

Table 3 shows the variation of the basic properties of the treated peaty clay after 28 days. According to Table 3, dry density is increased as the FA content is increased because of the higher specific gravity of FA compared with CCR and peat. Moisture content has been reduced when more and more CCR and FA are added since moisture is dissipated for the hydration process.

3.1 *Unconsolidated Undrained shear strength*

Strength improvement of the peaty clay with the increment of Calcium Carbide residue content is shown in the Fig. 4. The strength development can be classified in to three zones. Active zone- Strength is clearly increasing with the input of CCR. Inert Zone- Strength development gradually slow down since the amount of pozzolanic materials in the peat gets depleted. Deterioration Zone- Strength is decreased since no pozzolanic materials left and due to the unsoundness caused by free lime.

Both short term and longterm graphs show gradual deflections between 10-20% of CCR content. Up to 10% of CCR, ample amount of natural pozzolanic materials is available in the soil and after that it is get depleted however the deterioration zone is not met yet. Therefore, the graphs were extended using best fit (R^2> 0.99) polynomial trend line to observe the inert and the deterioration zones. This gives the idea of the capacity of the peaty clay to absorb Ca^{2+} ions which comes from $Ca(OH)_2$. The reaction of CCR with the soil particles occurs in three stages. Ca^{2+} ions get attracted to the negatively charged particles of peaty clay and replace cations of the soil known as cation exchange. This will make the soil particles to clump in to large sized particles and that is flocculation and aggregation. Hydrous Silica and hydrous Alumina of the soil dissolved due to OH^- medium react with Ca^{2+} and that is the pozzolanic reaction.

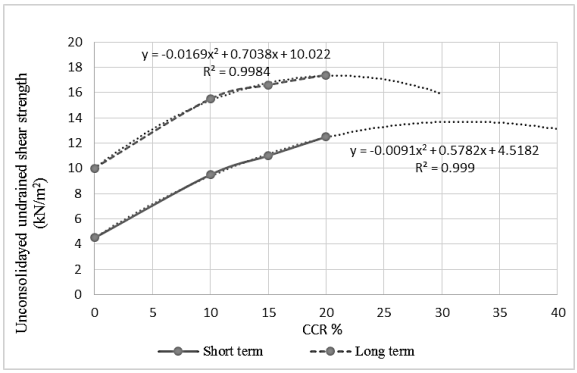

Fig. 4 UU strength of peaty clay with the CCR content

Fig. 5 shows unconsolidated undrained shear strength variations of peaty clay with and without mixing of additives.Peaty clay of very low shear strength of 5 kN/m^2 can be improved to 10 kN/m^2 by loading for 90 days which shows the effect of pre-loading method. CCR treated soil samples have comparatively less shear strength improvement in short term however can be made high with the time.

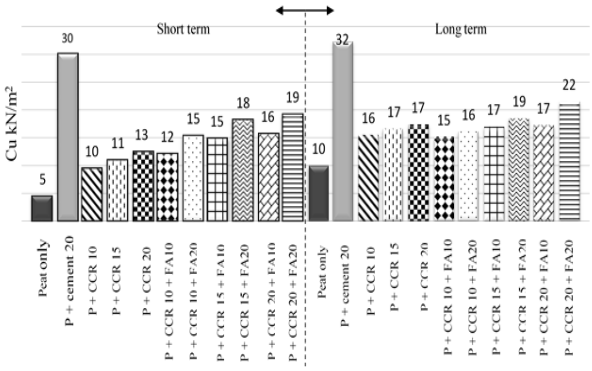

Fig. 5 C_u values of samples subjected to short term and longterm loading

Table 3. Basic Properties of treated peaty clay samples after 28 days

	Moisture Content (%)	Specific Gravity (Gs)	Bulk Density (kg/m^3)	Dry Density (kg/m^3)	Organic Content (%)	pH value
P	300	1.819	1104.0	196.0	40.5	2.3
P+C20	170	2.110	1211.9	448.9	21.2	11.4
P+CCR10	276	1.809	1162.3	309.1	28.9	11.5
P+CCR15	230	1.924	1193.0	361.5	25.8	11.7
P+CCR20	204	1.967	1190.9	391.8	22.1	12.1
P+CCR10+FA10	195	1.879	1187.0	402.4	29.5	12.9
P+CCR10+FA20	161	1.969	1249.4	478.7	22.5	13.4
P+CCR15+FA10	167	1.957	1244.4	466.1	19.7	11.5
P+CCR15+FA20	140	2.137	1254.9	522.9	19.5	11.3
P+CCR20+FA10	150	2.058	1268.0	507.2	18.7	11.1
P+CCR20+FA20	125	2.042	1309.0	581.8	18.6	11.4

Long term CCR 20% shows relatively high strength than many short term CCR + FA combinations since the peat contains high pozzolanic materials and having much time for Ca^{2+} ions to get attached with soil particles and to occur flocculation and thereafter the pozzolanic reaction.

CCR, FA combinations which indicate significant strength improvement in short term decline their rate of improvement afterwards, long term. The pozzolanic reaction occurs rapidly when both CCR and FA present and therefore rapid strength increment in short term. Even in the CCR, FA combinations the FA content governs the strength improvement. Packing effect of FA also contribute to the strength development.

3.2 *Microstructural variations*

Fig. 6 shows the irregular shape of the peaty clay particles. The voids among the particles are clearly depicted.When it comes to both CCR and FA mixed samples the spherical FA particles are covered by rod shaped structures and forms a well aggregated structure (Somna et al., 2011). The void nature that present in peaty clay cannot be seen in the Fig. 7.

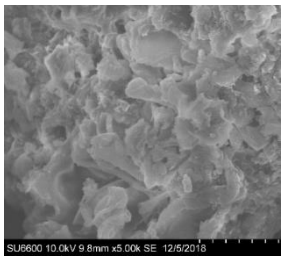

Fig. 6 SEM image of peaty clay

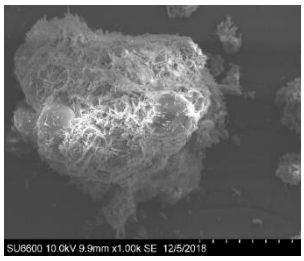

Fig. 7 SEM image of CCR, FA mixed peaty clay

4 CONCLUSIONS

Although cement is currently the best solution to stabilize peat, CCR and FA combination has shown considerable strength development in the present study. Fig. 8 shows a comparison of shear strength values of the treated peat with different materials by Madushanka (2015) and Maduransi (2015). Direct comparison can be done using the star marked results and the present study results. From the results it is evident that even withhigher moisture content and organic content, the peaty clay treated with CCR and FA have satisfactory strength improvements. Therefore, by adding or replacinga portion of CCR with little amount of cement (about 5%), a significant strength improvement can be expected.

However, coal fly ash consists of heavy metals (Ukwattage et al., 2016) which may cause for environmental and health risks when mixed with the nearby water bodies. Hence, an extensive environmental study on the effect of heavy metal leachability from fly ash during soil stabilization should be conducted before any industrial application.

ACKNOWLEDGEMENT

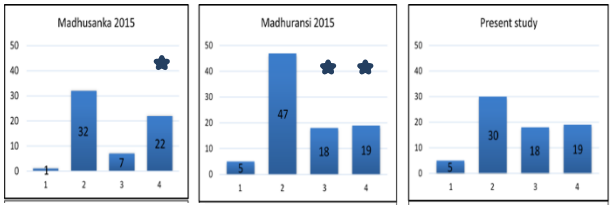

Madhusanka 2015	Madhuransi 2015	Present study
MC 300%, OC 22%	MC 290%, OC 22%	MC 400%, OC 40%
Gs 1.5	Gs 1.5	Gs 1.8
Applied stress 10kN/m^2	Applied stress 10kN/m^2	Applied stress 10kN/m^2
1-peat only	1-peat only	1-peat only
2 cement 20%	2 cement 30%	2 cement 20%
3 PHA 20%	3 PHA 10% + Cem 20%	3 CCR15% + FA20%
4 PHA15% +Cem 15%	4 PHA20% +Cem 10%	4 CCR20% + FA20%

Fig. 8Comparison of results with previous studies

The assistance given by laboratory staff of Geotechnical Engineering Division of Department of Civil Engineering, University of Moratuwa and the facilities provided by Sri Lanka Institute of Nanotechnology (SLINTEC) to obtain the SEM images of the samples are acknowledged.

REFERENCES

Horpibulsuk, S., Phetchuay, C., &Chinkulkijniwat, A. (2011). Soil stabilization by calcium carbide residue and fly ash. Journal of materials in civil engineering, 24(2), 184-193.

Kolay, P. K., &Pui, M. P. (2010). Peat stabilization using gypsum and fly ash. Journal of Civil Engineering, Science and Technology, 1(2), 1-5.

Madhusanka, S. K. (2015). Possible use of Paddy Husk Ash in Improvement of Engineering Characteristics of Peaty Clay.<http://dl.lib.mrt.ac.lk/handle/123/13157> (Dec. 5, 2018).

Madhuransi, L. W. I. (2015). Use of paddy husk ash as a binder in improvement of soft peaty clay.<http://dl.lib.mrt.ac.lk/handle/123/13160> (Dec. 9, 2018).

Nalbantoğlu, Z. (2004). Effectiveness of class C fly ash as an expansive soil stabilizer. Construction and Building Materials, 18(6), 377-381.

Somna, K., Jaturapitakkul, C., &Kajitvichyanukul, P. (2010). Microstructure of calcium carbide residue–ground fly ash paste. Journal of Materials in Civil Engineering, 23(3), 298-304.

Ukwattage, N. L., Ranjith, P. G., & Perera, M. S. A. (2016). Effect of accelerated carbonation on the chemical properties and leaching behaviour of Australian coal fly ash, to improve its use as a compost amendment. Environmental earth sciences, 75(21), 1398.

Venuja, S., Mathiluxsan, S., &Nasvi, M. C. M. (2017). Geotechnical Engineering Properties of Peat, Stabilized with a Combination of Fly Ash and Well Graded Sand. Engineer: Journal of the Institution of Engineers, Sri Lanka, 50(2).

Analysis of Stability Enhancement of Soldier Pile Retaining Wall

Athmarajah.G
Department of Civil Engineering, University of Moratuwa, Sri Lanka

ABSTRACT: In construction industry, Soldier pile retaining wall with timber laggings is one of the most common retaining walls. Stability of the soldier pile retaining wall is the main consideration during the design and construction period. To predict the lateral wall deformation for excavations, it is important to perform a numerical analysis, because the deflection of the soldier pile retaining wall is critical in practice. In the present study, theoretical analysis and numerical analysis were carried out to analyse the stability of the soldier pile retaining wall with the presence of surcharge. This research mainly focusing on the stability enhancement of the soldier pile retaining wall considering the factors such as, depth of embedment of the steel H-sections, spacing between steel H-sections, width of the steel H-section and soil parameters. Also, this paper presents the results of theoretical study using limit equilibrium method to assess the stability of the wall by considering the factor of safety. And, two-dimensional finite element model (FEM) of soldier pile retaining wall with horizontal timber laggings was created in Plaxis 2D software to estimate the lateral displacement of the wall.

1 INTRODUCTION

Soldier pile retaining wall is widely used as an excavation support in modern practices. The main advantages of using soldier pile retaining wall with horizontal timber laggings are cost effectiveness, fast construction and no advanced techniques required in the construction of the wall. However, as like advantages there are some drawbacks in soldier pile retaining wall such as unable to construct in higher ground water table because of the water penetration through the timber laggings, not much stiffer like other retaining walls such as steel sheet pile, secant pile wall, diaphragm walls and etc, possibility of ground settlement due to the poor backfilling or large lateral deformation [1].

2 OBJECTIVES

Objectives are to investigate the effect of depth of embedment and width of steel H-sections, spacing between steel H-sections, and different soil parameters on the stability enhancement of soldier pile retaining wall. Then develop some design charts to assist the design of soldier pile retaining walls considering the above factors by theoretical and numerical study.

3 LITERATURE REVIEW

Number of researches have been carried out to analyze the soldier pile retaining wall performance considering many factors that would affect the stability of the wall using experimental study and numerical analysis. Rashidi and Shahir (2017) investigated the performance of the anchored soldier pile in the presence of the surcharge by creating 3D numerical model using Abaqus software [2]. Chung-Jung Lee and Chen (2013) carried out an experimental study on a self-supported soldier pile wall in sandy soils to find out the reduction in surface settlement, maximum horizontal settlement, maximum tilting angle on the wall crest and the maximum bending moment [1]. Johari and Kalantari (2016) have analyzed the effect of rainfall infiltration and dynamic loads on soldier pile excavations by a numerical model using GeoStudio software [3].

Not only that, Hong and Lee (2003) performed a numerical study on three-dimensional pile-soil interaction in soldier piled excavations and found out deflection behind timber laggings and swelling and softening of soil face just behind the timber laggings by comparing the 2D and 3D results [4]. Also, Dharshan and Keerthi Gowda (2016) developed a Finite Element Model using SAP2000 to study stability enhancement of cantilever earth retaining wall with pressure relief [5].

4 METHODOLOGY

4.1 *General*

This study was performed mainly in two phases and results were compared at last. For both Limit Equilibrium analysis and Finite Element Modelling, material properties and soil parameters have been taken as same. And the surcharge is taken as 10 kN/m2 for all cases which is referred from BS 8002.The different analysis cases are shown below,

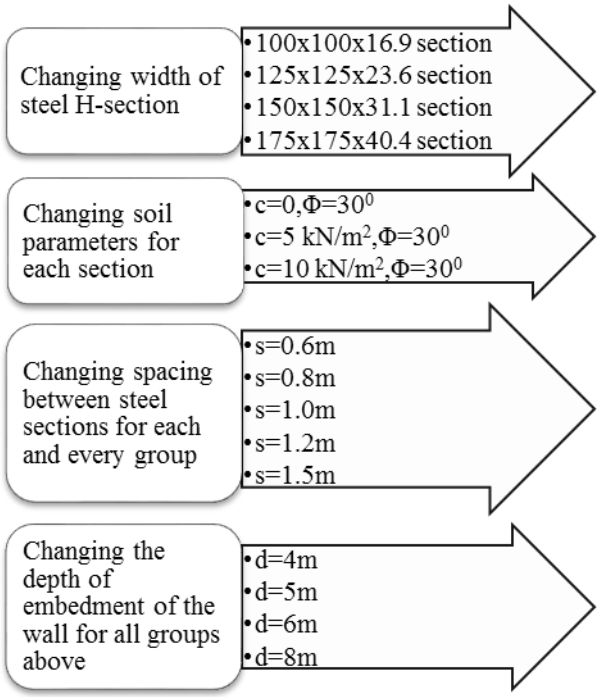

Figure 1-Methodology

4.2 *Limit Equilibrium analysis*

In the code of practices, analysis of the retaining wall is defined from limit equilibrium method. The analysis of soldier pile retaining wall with timber laggings is carried out like steel sheet piles. The model that considered for the analysis is presented below,

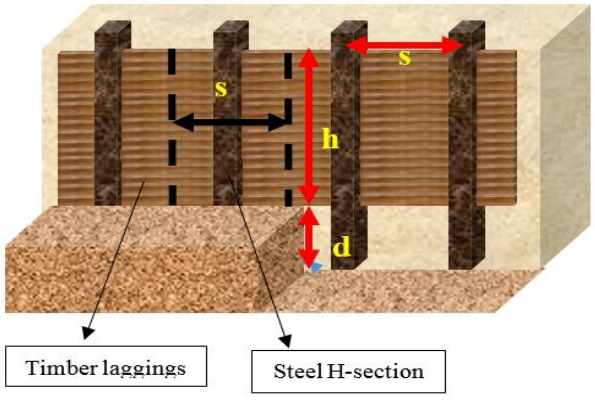

Figure 2-Geometric model of soldier pile wall

where, s- spacing between two steel H-section
h- retention height
d- depth of embedment

According to the Rankine and Coulomb theory, the forces on both active and passive sides along timber laggings and steel H-sections were considered for the limit equilibrium analysis (consider the distance of 's'which includes both timber lagging and steel section).

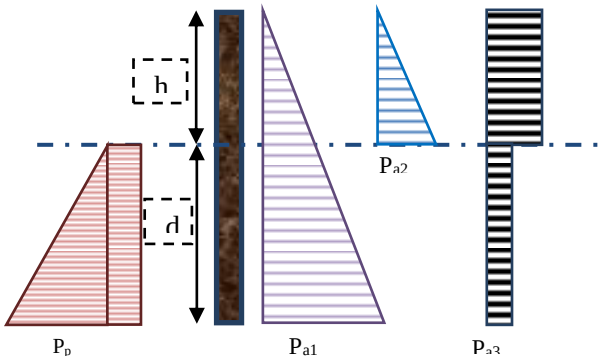

Figure 3-Pressure distribution diagram

where,
P_p-Passive pressure distribution
P_{a1}-Active pressure distribution along steel H-section
P_{a2}-Active pressure distribution along timber laggings
P_{a3}-Active pressure distribution along steel H-section and timber laggings due to surcharge

Also, Rankine proposed the coefficients to be,

$$K_a = (1-\text{Sin }\Phi)/(1+\text{Sin }\Phi) \quad (1)$$

$$K_p = (1+\text{Sin }\Phi)/(1-\text{Sin }\Phi) = 1/K_a \quad (2)$$

Finally, moment equilibrium has been considered to find out Factor of Safety (FoS) for each case like,

Overturning moment,

$$M_0=\{P_{a1}x(d+h)/3\}+\{P_{a2}x(d+h/3)\}+ \{(qK_a)xW_sxdxd/2\}+\{(qK_a)xsxhx(d+h/2)\} \quad (3)$$

Restoring moment,

$$M_R=\{(\gamma dK_pxd/6)+(2c\sqrt{K_p}xd/2)\}xdxWs \quad (4)$$

Factor of safety,

$$FoS= M_R/M_o \quad (5)$$

where,
K_p-Passive pressure coefficient
Ka-Active pressure coefficient
W_s-Width of the steel H-section
c-Cohesion of soil
Φ-Friction angle of the soil

4.3 *2-Dimensional Finite Element Modelling (FEM)*

In order to develop a numerical model, to replicate the performance, Plaxis 2D software was used in this study. The soldier pile and timber laggings were idealized as two-dimensional plain strain model and plastic analysis has been used for the analysis.

5 MATERIAL AND SOIL PROPERTIES

Table 1- Properties of soil

Φ	300
E (kN/m2)	17000
γunsat (kN/m3)	18
γsat (kN/m3)	20
v	0.3
Rinter	0.67

Table 2 – Properties of timber

Timber (50mmx100mm)	
A(mm^2)	50xspacing
I(mm^4)	1000x50^3/12
E(N/mm^2)	10300
ρ(kg/m^3)	540
w(kg/m)	2.7
v	0.35

Table 3 – Properties of steel H-sections

	A (cm^2)	I (cm^4)	w(kg/m)	E (GPa)	v
100x100x16.9	21.59	378	16.9	210	0.3
125x125x23.6	30	839	23.6		
150x150x31.1	39.65	1620	31.1		
175x175x40.4	51.43	2900	40.4		

6 RESULTS AND DISCUSSION

6.1 *Limit Equilibrium analysis results*

In Figure (4), Factor of Safety of the soldier pile wall obtained from the equation (5) plotted against the depth of embedment for various spacings between steel H-sections for sandy soils (c=0, $\Phi=30^0$). It can be seen that, for the walls with higher depth of embedment that the FoS becomes larger. Not only that, it is clear that the factor of safety values are reducing when the spacing between steel H-sections becomes closer or smaller.

The variation of factor of safety against the depth of embedment for various soil types for the spacing between steel H-section of 1.5m is shown in Figure (5). The variations clearly indicate that the factor of safety values are increasing with the increase in cohesion of the soil.

In Figure (6), factor of safety varies with the variations of spacings between steel H-sections and width of the steel sections for the depth of embedment 5m and for the soil having c=5 and $\Phi=30^0$. The graph shown below clearly describes that the values of factor of safety increases for the larger steel H-sections.

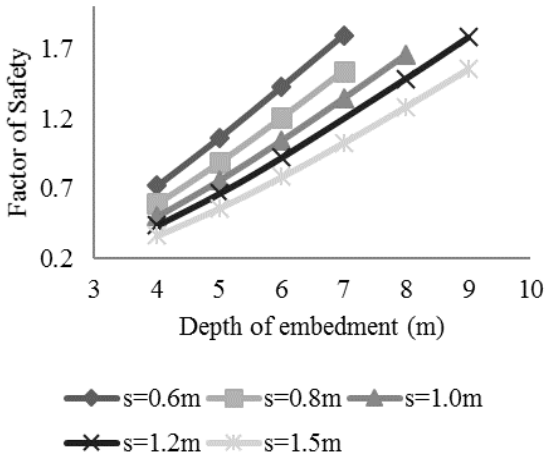

Figure 4- Variation of factor of safety with depth of embedment and spacing between steel H-section

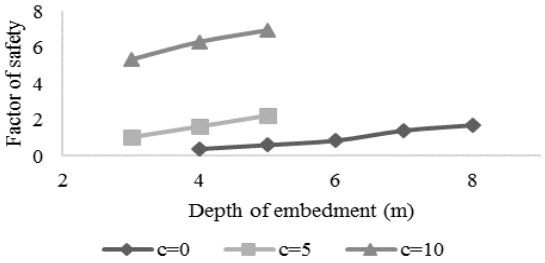

Figure 5- Variation of factor of safety with spacings between steel H-sections and different soil types

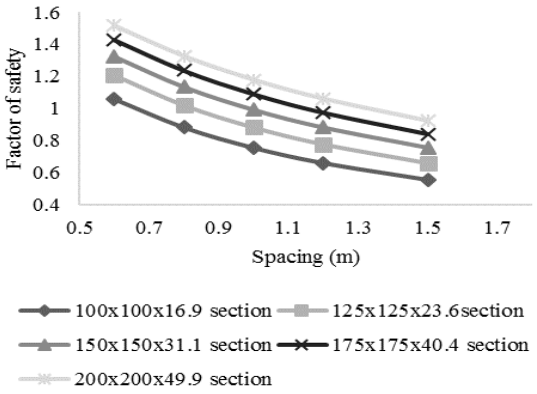

Figure 6- Variation of factor of safety with spacing and width of steel H-section

6.2 *Two dimensional Finite Element Modelling (FEM) Results*

The below Figure (7) signifies the lateral displacement of the soldier pile variations against the depth of embedment of the wall for various spacings for the soil having parameters of $c=10kN/m^2$ and $\Phi=30^0$. It can be clearly realized that; the wall displacements are increasing when the depths of embedment are smaller. Also, for particular depth

of embedment of steel H-section, the displacement of the wall is increasing for larger spacings between steel H-sections.

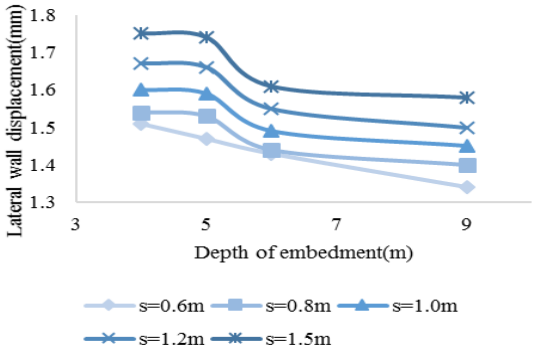

Figure 7- Variation of lateral wall displacement with depth of embedment and spacings between steel H-sections

In Figure (8), lateral wall displacement of the wall is plotted against the depth of embedment for various soil types for the spacing between steel sections of `1.0m. It can be seen that, the wall displacements are reducing with the increment of cohesion of soil

The variation of lateral wall displacement with various width of steel H-sections and spacings between steel sections for the depth of embedment 8m and soil having properties of c=10 kN/m^2 that described in Figure (9) below. The graph shows that the wall displacement reduces for the larger steel H-sections.

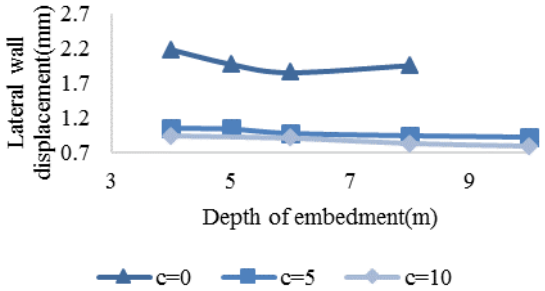

Figure 8- Variation of lateral wall displacement with depth of embedment and different soil types

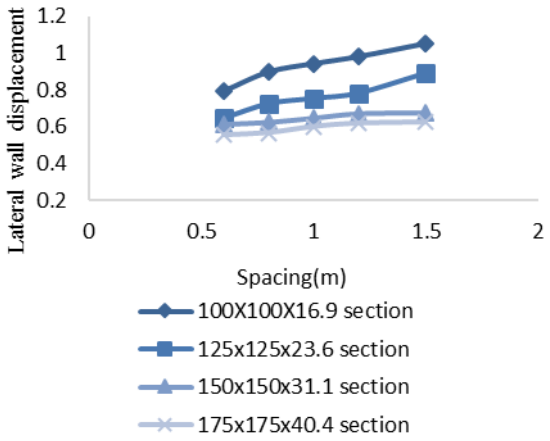

7 CONCLUSION

The results from both limit equilibrium analysis and 2-dimensional Finite Element modelling were compared and concluded. The main findings of this study are as follows,

- The stability of the soldier pile retaining wall with timber laggings is enhanced by increasing the depth of embedment of the wall.
- Increasing the spacing between steel H-sections reduces the stability of soldier pile wall significantly.
- The width of the steel sections strongly influences on the stability enhancement of the soldier pile wall with timber laggings.
- Also, the stability of the wall depends on the stiffness on the soil. Soldier pile retaining wall with horizontal timber laggings is more stable in stiffer soils.

ACKNOWLEDGMENTS

The author is very thankful to Dr.L.I.N.De Silva who gave full support and guidance to complete this study successfully.

REFERENCES

1] Chung-Jung Lee, Yu-Chen Wei, Huei-Tsyr Chen, Yu-Yi Chang, Yi-Chian Lin and Wen-Shi Huang, “Stability analysis of cantilever double soldier-piled walls in sandy soil,” Journal of the Chinese Institute of Engineers, vol. 34, p. 449–465, June 2011.

2] F. Rashidi and H. Shahir, “Numerical investigation of anchored soldier pile wall performance in the presence of surcharge,” International Journal of Geotechnical Engineering, 2017.

3] A.Johari and A.R.Kalantari, “Evaluation of rainfall infiltration and dynamic loads effects on soldier piled excavation,” International Conference on Geotechnical Engineering and Soil Mechanics, 15-17 November 2016.

4] F. L. K. Y. S.H. Hong, “Three-dimensional pile-soil interaction in soldier-piled excavations,” Computers and Geotechnics, vol. 30, p. 81–107, 2003.

5] K. G. B. S. Dharshan K, “Stability Enhancement of Cantilever Earth Retaining Wall with Pressure Relief Shelf by Soft Computing Technique,” Advanced Engineering and Applied Sciences: An International Journal, pp. 65-68, 2016.

Study on Development of Arching Action of Sand Using an Earth Pressure Cell

E. Havisanth
Department of Civil Engineering, University of Moratuwa, Sri Lanka

ABSTRACT: Stress transformation from yielding part of soil on to adjacent rigid part is known as the arching action of soil. Stresses acting on underground structures need to be estimated correctly for economical design and evaluation of the performance of those structures accounting the effect of soil arching. An experimental approach in measuring real-time stress variation on buried structures due to arching effect of soil is discussed in this paper. Experimental study was done to study the effect of both active and passive soil arching in dry and saturated sandy soil using effective & total earth pressure cells and the stress variation on underground structures was analyzed. Results conclude that in passive soil arching stress transform to structures increase with stress increment where, as the stress transform to structures reduce with settlement of the structure. In addition, settling of surrounding soil causes increase in the stress transform to structures.

1 INTRODUCTION

Phenomenon of stress transformation from yielding part of soil onto adjacent rigid part is known as the arching action of soil (Terzaghi.K, 1943), which is encountered in both underground structures and natural terrains. Arching occurs when there is a difference of the stiffness between the installed structure and the surrounding soil. If the structure is stiffer than the soil, then loads arches onto the structure. Otherwise, if the structure is less stiff than the soil then loads arches away from the structure.

Depending on relative stiffness of surrounding soil mass, arching phenomenon tends to have both positive and negative impacts on underground structures, hence the arching action can be either active or passive. Reduction of overall stress transformed on to structure from overlying soil is the foremost positive impact of arching effect. This occurs when surrounding soil around a structure is stiffer than the structure and this is known as active arching. Increase of stress transformed to the structure is the foremost negative impact of soil arching which occurs when structure is stiffer than the surrounding soil mass (Evans, 1984).

2 PROBLEM STATEMENT

Necessity of evaluating the stresses acting on underground structure is a key issue in geotechnical designs, since construction and maintenance of those structures cost much than regular structures. Present theories and method to estimate stresses accounting arching effect are either time consuming or approximate evaluations, this causes the need for new methods to correctly evaluate/estimate arching effect. This research was carried out with the intention of studying the development of soil arching using earth pressure cells experimentally.

3 THEORETICAL EVALUATION OF ARCHING ACTION OF SOIL

Governing equation to determine vertical stress (σv) on yielding strip below soil mass considering arching action of soil proposed by Terzaghi (Terzaghi.K, 1943)can be written as follows:

$$\sigma_v = \frac{B(\gamma - c/B)}{K \tan\varphi}(1 - e^{-K*n*\tan\varphi}) + q * e^{-K*n*\tan\varphi} \quad (1)$$

$$n = z/B \quad (2)$$

Terms in (1) & (2) are; 2B = width of yielding strip, z -depth, γ -unit weight of soil, σv -vertical stress, K-coefficient of lateral stress, c-cohesion, φ -friction angle, q-surcharge applied.

4 METHODOLOGY

Study was done in four main phases,

- Development of total and effective earth pressure cells to measure soil pressure
- Modelling of experimental setup with earth pressure cells to study development of soil arching
- Experiments and data collection
- Study and evaluation of development of soil arching using experimental results

4.1 *Modelling of experimental setup*

Experimental setup to study passive soil arching effect in dry soil – setup was modelled with con-

crete block (150mm×150mm×150mm) placed at the mid of circular clay layer (outer diameter 710mm, height 150mm, thickness 140mm) formed at the center of plastic container, space between the concrete block and clay layer was filled with sandy soil used in the experiment (refer to Fig. 1). Concrete block was modelled to be a rigid structure than surrounding soil.

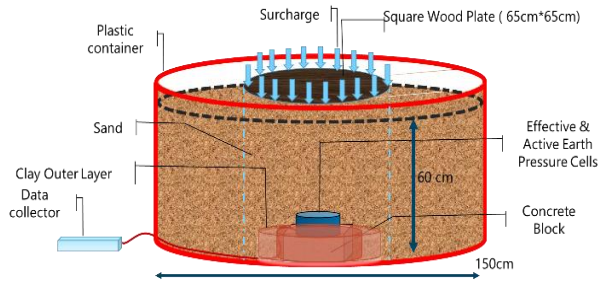

Fig.1 Experimental model to study passive soil arching

Clay block (58cm×28cm×20cm) made of clay near to liquid limit was placed at the center of container instead of concrete block to model active arching in sand. Clay block was modelled to be a flexible structure than surrounding soil.

Experimental setups to study arching effect with known settlement and increments in dry sand - other than above setups were modelled by creating a trapdoor setup with 2-ton scissor jack.

Fig.2. Two ton scissor jack (Trapdoor)

5 RESULTS AND DISCUSSION

5.1 *Basic soil properties*

Fig 3 presents particle size distribution of sandy soil used in experiments, done using dry sieve analysis based on ASTM D422 standards.

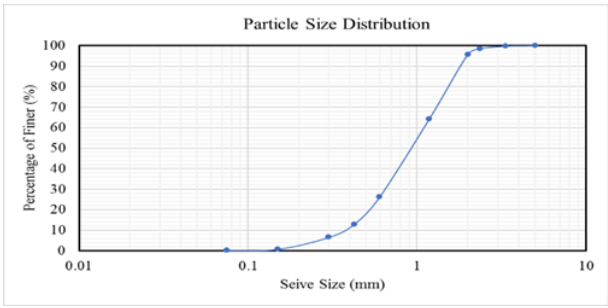

Fig.3 Particle size distribution curve

From the sieve analysis results coefficient of curvature of sand is 0.78 and coefficient of uniformity of this sand is 2.45. Used sand sample can be categorized as poorly graded sand following the Unified Soil Classification System.

Direct shear test was done based on ASTM D3080 standard to determine the friction angle of sandy soil used. From the direct shear test friction angle of soil is found to be 340.

5.2 *Passive soil arching in dry sand*

Variation of stress measured with time using the earth pressure cell placed on concrete block with applied surcharge on the setup is shown in Fig. 4.

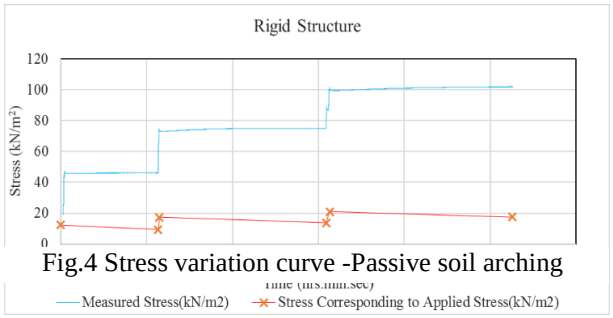

Fig.4 Stress variation curve -Passive soil arching

Fig. 4 shows that stress measured by earth pressure cell is greater than the corresponding applied stress at the sensor level considering 2:1 stress distribution in the soil fill. This increase in measured stress is due to the development of passive soil arching since the concrete block is relatively stiffer the surrounding soil. With the increase in applied stress it can be observed that difference in measured stress and applied stress increases, which shows that effect of development of passive soil arching increases with applied stress.

5.3 *Active soil arching in dry sand*

Variation of stress measured using the earth pressure cell placed on top of the clay block is shown Fig. 5, which shows that the measured stress by the earth pressure cell is less than the corresponding applied stress at the sensor level due to development of active soil arching. With increase in applied stress it can be observed that the difference in measured stress and applied stress increases, which shows that the effect of active soil arching increases with increase in applied stress.

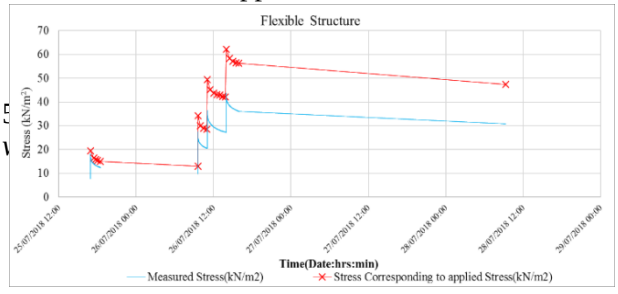

Fig.5 Stress variation curve – Active soil arching

From the fig 6 it can be observed that with the settlement of the structure the amount of stress measured by the earth pressure cell reduces. This is due to the development of active soil arching when the relatively stiff structure settles with respect to the surrounding soil. But all these measured stresses during the whole set of experiments remains to be greater than the corresponding applied stress at the sensor level. This is because of development of passive soil arching due to greater relative stiffness of the structure comparing to surrounding soil.

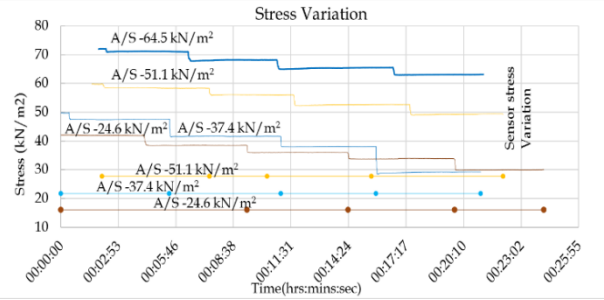

Fig.6 Variation of applied stress & measured stress with time

5.4.1 Interpretation of active arching experimental results

Reduction in measured stress with applied stress corresponding to different amount of trapdoor settlements are graphically represented in the Fig. 7. From these figures, reduction in stress transformed on to the structure considering development of arching effect can be obtain for the structure

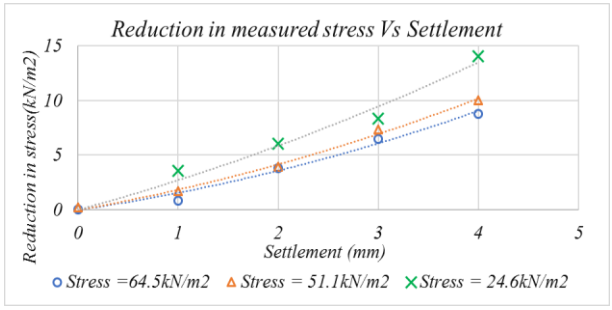

Fig.7 Reduction in measured stress with settlement of the structure

5.5 *Evaluation of development of passive arching with a known relative settlement of sand*

From the fig 8 it can be observed that with relative settlement of surrounding soil in response to structure, amount of stress measured by the earth pressure cell increases. This is due to the development of passive soil arching. It can be also observed that with the increase in applied stress, the amount stress transformed on to the structure reduce Observed step increase in the measured stress are during the increment of height of the structure by each 1mm.

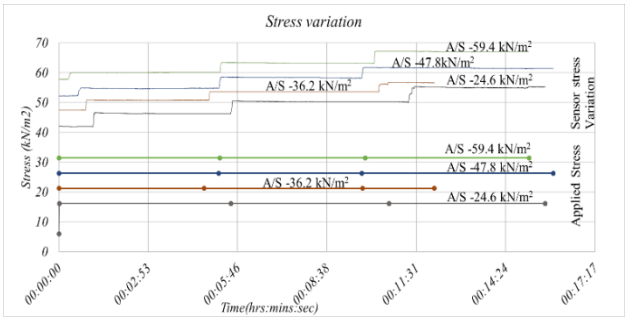

Fig. 8 Increase in measured stress with applied stress

Fig. 9. Presents the increase in stress transformed on to the structure with relative settlement of surrounding sand for various applied stress.

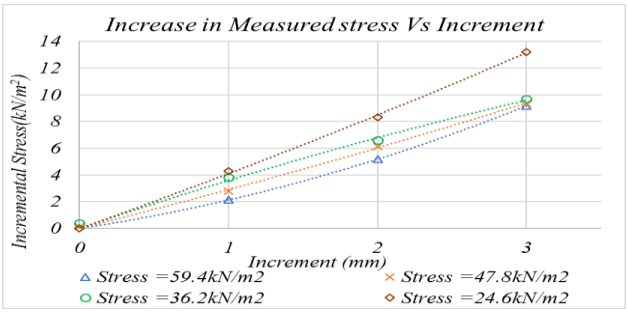

Fig. 9Increase in measured stress with applied stress

6 COMPARISON OF EXPERIMENTAL RESULTS WITH THEORETICAL EVALUATION

Results obtained during active soil arching (experiment using clay blocks) and experimental results obtained using the trapdoor were compared to the results of theoretical evaluation using Terzaghi's equations on soil arching developed based on trapdoor test. Stress values obtained from the experiment shows that similar variation of values compared to theoretical evaluation. Both stress values are less than the actual applied stress on the setup. Meanwhile stresses measured by sensors are slightly less than the values estimated theoretically. Fig. 10 represents the theoretical comparison results.

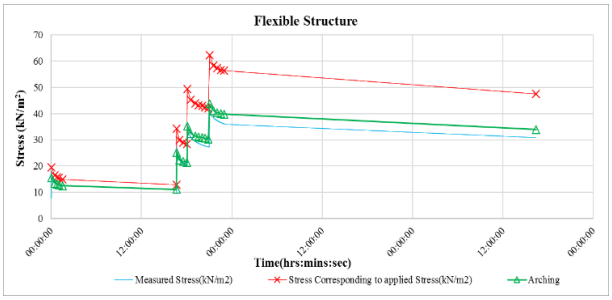

Fig. 10 Variation of experimental results & Theoretical evaluation

Fig. 11 interprets that the stress values measured by sensor immediately after applying the stress to the setup is greater than the stress estimated theoretically. However, with the settlement of the trapdoor, the measured stress values approach the theoretically estimated values.

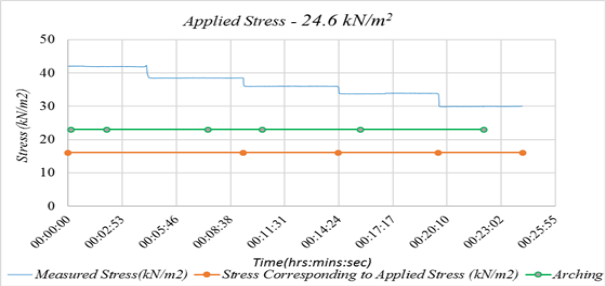

Fig. 11 Comparison of experimental result with theoretical value

7 CONCLUSIONS

Rigid body experiment - It can be concluded that stress increment on a rigid structure during development of passive soil arching increases with the stress applied.

Flexible structure experiment -In active soil arching with increasing applied stress the rate of reduction in stress transformed on to the structure increases.

Trapdoor experiment (dry sand) -For an applied constant stress, measured stresses reduces with the settlement of the structure due to the development of active soil arching. Reduction in stress during settlement of structure depends on the amount of settlement, saturated condition and applied stress on the structure. Amount of stress reduction decreases with increasing applied stress.

Table 1. Stress reduction for each 1mm settlement

Applied Stress (kN/m^2)	Stress Reduction (kN/m^2)
25 -35	2.8
35-45	2
45-55	1.8
55-65	1.5

Table 1 represents the stress reduction approximately for 1mm change in settlement, for δ/B =1/230, H/B=1.96 (where δ-settlement, B- width of the structure, H- height of soil fill)

Fig. 12 shows the variation of required settlement needed for attaining the full mobilization of soil arching.

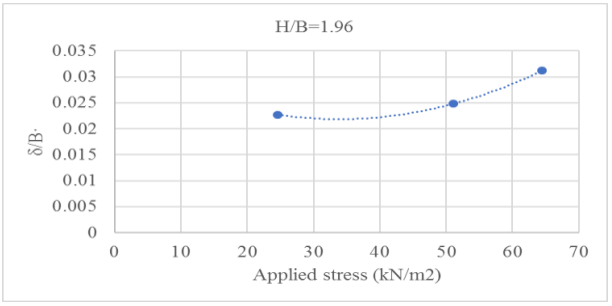

Fig. 12 Settlement required for full mobilization of soil arching

Increment in height of rigid body experiment (dry sand) -This concludes that stress transformed on to the structure increases when the surrounding soil settles relative to the structure. Amount of stress increase decreases with increasing applied stress.

Table 2. Stress increment for each 1mm relative settlement of sand

Applied Stress (kN/m^2)	Stress Increment (kN/m^2)
25-35	4
35-45	3.4
45-55	3
55-65	2.8

Table 2 represents the stress increase approximately for 1mm increase in height of structure, for δ/B =1/230, H/B=1.96.

ACKNOWLEDGEMENT

The author wishes to acknowledge the assistance and guidance given by the Supervisor of undergraduate research. Finally, author would like to convey gratitude to Department of Civil Engineering and its staffs of University of Moratuwa.

REFERENCES

Evans, C. (1984). *An examination of arching in granular soils.* Massachusetts Institute of Technology.

Handy.L, & Richard. (March 1985). The Arch in Soil Arching. *Journal of Geotechnical Engineering 111(3)*, 302-318.

Mckelvey, & James. (1994). The anatomy of soil arching. *Geotextiles and Geomembranes 13(5)*, 317-329.

Terzaghi.K. (1943). *Theoretical soil mechanics.* London: John Wiler and Sons,INC.

Tien, & Hsien-Jen. (1996). *A Literature Study of the Arching Effect.* Massachusetts Institute of Technology, Dept. of Civil and Environmental Engineering.

An Experimental Investigation on Shaft Resistance of Cast In-situ Bored Piles in Intact Rock

S.Suloshini
Department of Civil Engineering, University of Moratuwa, Sri Lanka

ABSTRACT: Pile foundations are used to transfer the loads from large structures to underlying bedrock when the surface soils are unable to provide adequate bearing capacity. The bearing capacity of pile foundation depends on base resistance and shaft resistance. The shaft resistance of pile is a very sensitive parameter and governed by several parameters. This research is focused on the experimental investigation on shaft resistance of cast in situ bored piles in intact rock. The ultimate shaft resistance was calculated from the experimental results for different rocks commonly found in Sri Lanka such as biotite hornblende gneiss, marble rock and charnokitic hornblende gneiss. It was found that these rocks have ultimate shaft resistance in the range of 3.5 - 4.5MPa and Shear modulus to be in the range of 60 – 70MPa. Confining stresses in the range of 0kPa to 400kPa do not seem to have any effect on the shaft resistance.

1 INTRODUCTION

Shaft resistance is an important component when calculating the bearing capacity of piles because it is mobilized earlier than the base resistance for a very small movement. The investigation of shaft resistance of pile – rock interface is a complex problem because it involves many factors such as mechanical properties of the surrounding rock, rock mass classification, pile diameter, roughness of rock – concrete interface, discontinuities of the rock, the radial force induced by the load applied on the pile and rock types . In normal practice the shaft resistance is estimated mainly using empirical methods. This might lead to very conservative estimation of ultimate shaft resistance of rock.

In view of the above the main objective of this study is to investigate the shaft resistance of cast in situ bored piles in intact rock through laboratory experiments.

2 LITERATURE REVIEW

From the literature it was noticed that several studies have been carried out on the shaft resistance of piles all over the world. The researches about the shaft resistance were commenced around 1950's. Before this period piles were designed by Terzaghi (1943) equation allowing for base resistance only and the shaft resistance was ignored in the design process due to lack of knowledge about the shaft resistance of rock socketed piles (Charif, Najjar, & Sadek, 2010).

Later it was realized that the shaft resistance is a significant parameter when designing the rock socketed piles. Specific allowance for shaft resistance in rock sockets started to appear in the mid 1960s. Values of allowable shaft resistance between 100 kPa and 1000 kPa were quoted for different rocks (Thornburn, 1966). Field load testing of rock socketed piles was possible in the early eighties.

Numerous studies were carried out to relate the shaft resistance with the unconfined compressive strength of surrounded rock. Many empirical correlations were proposed by the researchers to estimate the shaft resistance of rock-pile interface. Several available correlations to estimate the shaft resistance are stated in table 1 below (Charif et al., 2010; Thornburn, 1966).

Table 1. Empirical correlations for shaft resistance

Year	Correlation	Ultimate shaft resistance (fs)
1976	Rosenberg and Journeaux	$0.375(\sigma r)^{0.51}$
1979	Horvath and Kenney	$(0.2\text{-}0.3)(\sigma r)^{0.5}$
1981	Williams and Pells	$\alpha\beta\sigma r$
1987	Rowe and Armitage (Regular)	$0.375(\sigma r)^{0.5}$
	Rowe and Armitage (Rough)	$0.60(\sigma r)^{0.5}$
1987	Carter and Kulhawy	$0.15\sigma r$
1998	Zhang and Einstein (Smooth)	$0.40(\sigma r)^{0.5}$
	Zhang and Einstein (Rough)	$0.80(\sigma r)^{0.5}$
1999	O'Neill and Reese (IGM)	$\alpha\Psi\sigma r$

where,
σr – Unconfined compressive strength
α,β, Ψ – Parameters depending on various factors

The results got from the study of Charif et al (Charif et al., 2010) and another study of Rezaza-

deh and Eslami (Rezazadeh & Eslami, 2017) indicated that the relationship proposed by Horvath and Kenny (1979) provides the most reliable estimation of shaft resistance. Based on the findings of Ng et al (Ng, Yau, Li, & Tang, 2001) it was concluded that the magnitude of the shaft resistance is higher in the sedimentary rock than the granitic and volcanic rocks.

The maximum shaft resistance of concrete – lightly weathered silty mudstone was found as 1465 kPa by Tang et al (Hu, Tang, & Zhang, 2013). Shoib et al.(Shoib, Rashid, & Armaghani, 2017) have found that the ultimate rock shaft resistance in Malaysian decomposed granite can develop up to 1855 kPa. The maximum shaft friction of pile – marble interface was estimated as 300 kPa by Li et al. (Li, Wong, Yim, & Leung, 2011).

The significant increase in knowledge of rock socketed pile performance has led to the development of computer programs to calculate the load–deformation performance of socketed piles. A computer program Rocket has been developed and can be used for modelling. (Haberfield, 2011).

3 METHODOLOGY

3.1 *Sample preparation*

Cylindrical rock samples were cut at an angle of 60° with horizontal. From the τ-σ relationship it can be notified that the failure plane will occur at about 60° to the horizontal if the friction angle of rock is assumed as 30°. Here the rock-concrete interface is oriented in the same direction of the approximate failure plane.

Concrete grade was selected as G25. It is assumed that the strength of concrete does not affect the shaft resistance of rock – concrete interface because failure will occur along the rock – concrete interface. Testing was conducted for totally five samples including two samples of Biotite hornblende gneiss (A & D), a marble rock (C) and two samples charnokitic hornblende gneiss (B & E).

Fig. 1 Different types of rock samples

3.2 *Testing*

All the specimens were loaded after 28 days of curing as detailed below.

i. Step 01:-

Testing in triaxial apparatus at 400 kPa cell pressure

- Cycle 1:- First load the specimen up to 275 kN/m^2 of shear stress and then unload to zero.
- Cycle 2:- Load the specimen up to 550 kN/m^2 of shear stress and unload to zero.
- Cycle 3:- Load the specimen up to 1090 kN/m^2 of shear stress and then unload to zero. (Repeat this for two cycles)
- Repeat step 01 at 200kPa and 0kPa cell pressure

ii. Step 02:-

- Testing in UCS apparatus - Apply the load slowly (5.3 kN/sec) until failure

3.3 *Calculation of shaft resistance*

Calculation of stresses is illustrated in Fig. 2.

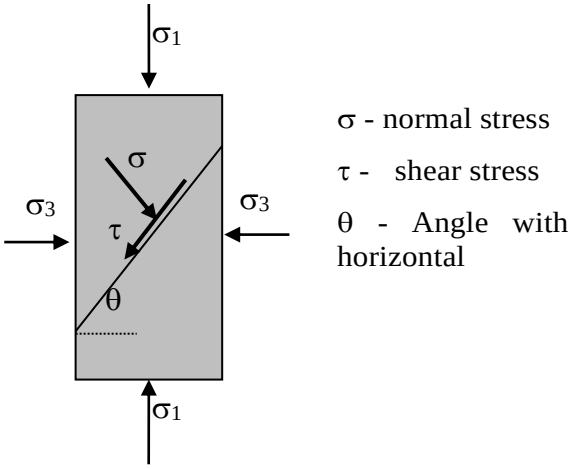

Fig. 2 Stresses acting on sample

$$\sigma = \frac{\sigma_1 + \sigma_3}{2} + \frac{\sigma_1 - \sigma_3}{2}\cos(2\theta) \quad (1)$$

$$\tau = \frac{\sigma_1 - \sigma_3}{2}\sin(2\theta) \quad (2)$$

4 RESULTS AND DISCUSSION

All five samples were tested in tri-axial apparatus at different confining pressures. All five samples did not fail in the tri- axial apparatus even at very high load (7 kN). Therefore tri-axial testing was stopped because it exceeds the capacity of the machine and testing was continued in UCS apparatus. Figs. 3 to 5 show the results obtained from tri-axial test at 400 kPa, 200 kPa & 0 kPa confining pressure of sample A (rock type - Biotite hornblende gneiss). And Figs. 6 to 9 show the results from tri-axial test for different types of rock samples.

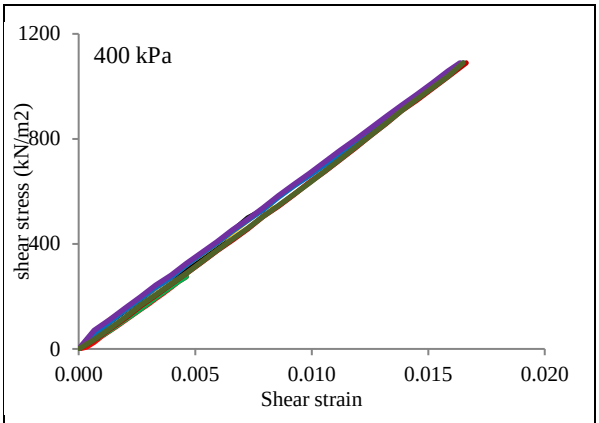

Fig. 3 shear stress – shear strain graph at 400 kPa

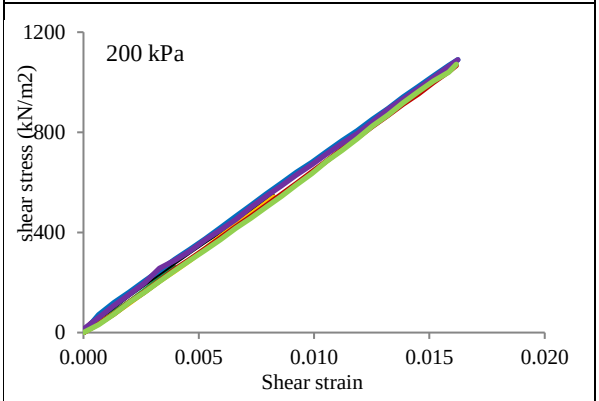

Fig. 4 shear stress – shear strain at 200 kPa

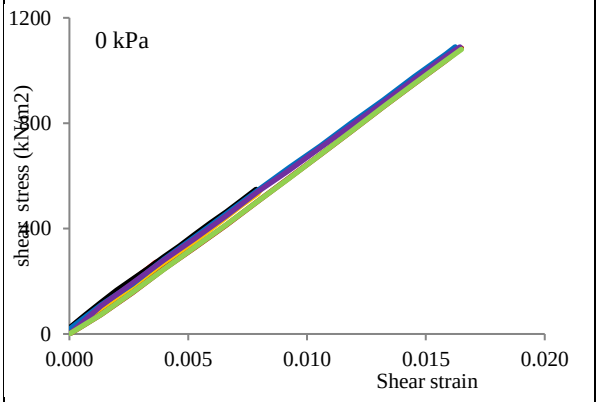

Fig. 5 shear stress – shear strain at 0 kPa

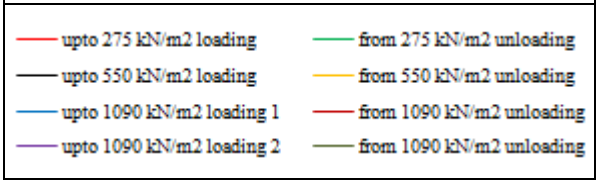

From these graph it can be clearly seen that the shear stress – shear strain behavior is more elastic with different loading and unloading patterns. The shear stress – shear strain follows almost similar behavior at different confining pressure (400 kPa, 200 kPa & 0 kPa). From this it can be concluded that the tested confining pressure range does not have significant effect on shaft resistance.

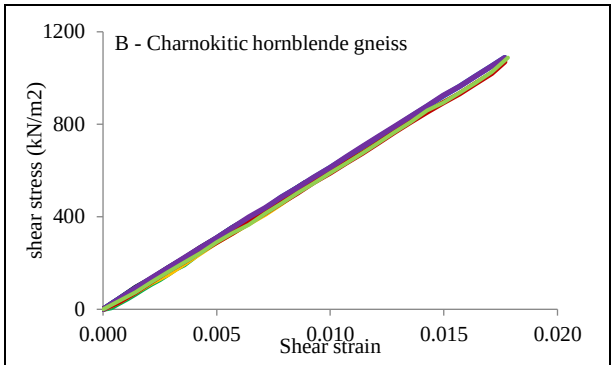

Fig. 6 shear stress – shear strain of charnokitic hornblende gneiss

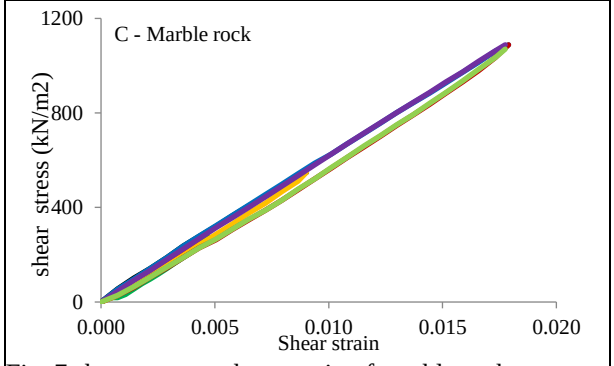

Fig. 7 shear stress – shear strain of marble rock

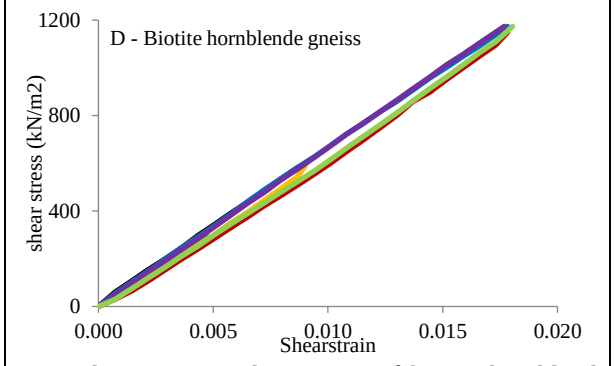

Fig. 8 shear stress – shear strain of biotite hornblende gneiss

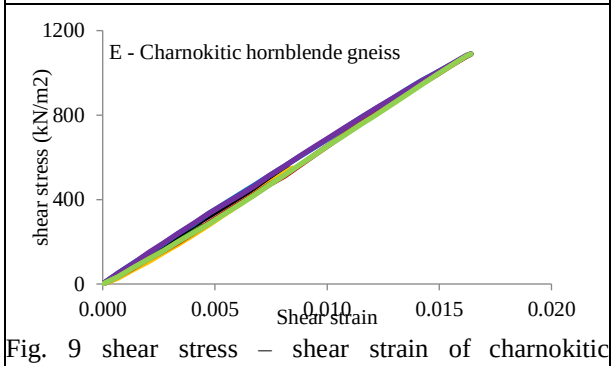

Fig. 9 shear stress – shear strain of charnokitic hornblende gneiss

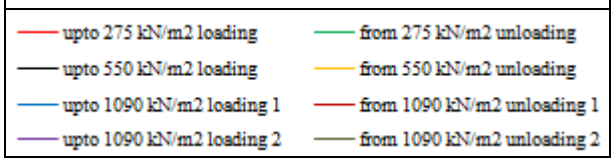

Ultimate shaft resistance and shear modulus of samples were calculated as shown in Table 2.

Table 2. Ultimate shaft resistance and shear modulus

Sample	Rock type	Ultimate shaft resistance (kPa)	Shear modulus of rock concrete interface (Mpa)
A	Biotite hornblende gneiss	3365	66
B	Charnokitic hornblende gneiss	4833	62
C	Marble rock	4216	61
D	Biotite hornblende gneiss	3364	67
E	Charnokitic hornblende gneiss	4006	67

The failure of all samples occurred along the rock – concrete interface as expected (refer to Fig. 10). But in the second sample B the failure occurred along the rock – concrete interface and within the rock due to discontinuity.

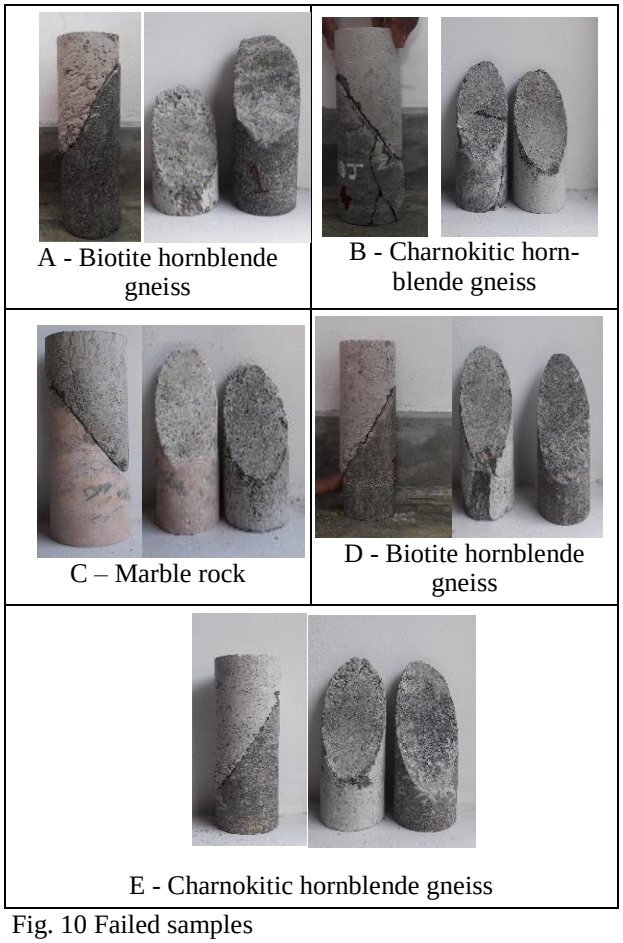

Fig. 10 Failed samples

Sample A and sample D are of same rock type (biotite hornblende gneiss) and their ultimate shaft resistance is also similar to each other. Sample B and sample E also with same rock type (charnokitic hornblende gneiss) but they have different shaft resistance. It may be due to the location variation and variation in properties of rock.

5 CONCLUSION

From the Shear stress - shear strain graph it can be stated that the behavior of the sample is more linear elastic with different loading and unloading cycles. The results obtained at different confining pressures are quite similar. From this it can be concluded that confining pressure does not have much effect on the shaft resistance of the rock – concrete interface within the tested stress range.

The findings of the research as follows, the ultimate shaft resistance of

- Biotite hornblende gneiss is 3365 kPa
- Marble rock is 4216 kPa
- One Charnokitic hornblende gneiss sample is 4832kPa and other sample is 4006 kPa.

Shear modulus of rock – concrete interface is found to be varying between 61 – 67 MPa for the tested specimens. The results got from this experiment can be used as a reference for designing the cast in-situ bored piles in rock under similar conditions.

ACKNOWLEDGMENTS

First of all I gratefully thank to my research supervisor Dr. L.I.N. de Silva for supporting and guiding me well. My heartiest thank to all the technical staffs of the geotechnical and building material laboratory for sacrificing their valuable time.

REFERENCES

Charif, K. H., Najjar, S. S., & Sadek, S. (2010). Side Friction along Drilled Shafts in Weak Carbonate Rocks. *Art of Foundation Engineering Practice*, 190–205.

Haberfield, C. M. (n.d.). *Rock-socketed pile design and construction: a better way?*

Hu, H., Tang, M., & Zhang, C. (2013). *Experimental study on side friction of uplift bored piles in soft rock*. *405-4.0*, 248–251.

Li, W. W., Wong, C. T., Yim, K. P., & Leung, M. K. (2011). Shaft resistance between marble and concretein rock-socketted large diameter bored pile: A review of state of art. *Procedia Engineering*, *14*, 1752–1758.

Ng, C. W. W., Yau, T. L. Y., Li, J. H. M., & Tang, W. H. (2001). Side resistance of large diameter bored piles socketed inti decomposed rocks. *Journal of Geotechnical and Geoenvironmental Engineering*, *127*.

Rezazadeh, S., & Eslami, A. (2017). Empirical methods for determining shaft bearing capacity of semi-deep foundations socketed in rocks. *Journal of Rock Mechanics and Geotechnical Engineering*, *9*(6), 1140–1151.

Shoib, R. S. N. S. R., Rashid, A. S. A., & Armaghani, D. J. (2017). Shaft resistance of bored piles socketed in Malaysian granite. *Proceedings of the Institution of Civil Engineers*, *170*(GE4), 335–352.

Thornburn, S. (1966). Large diameter piles founded in bedrock. *Proceedings of the Symposium on Large Bored Piles ICE*, 95–103.

Enhancement of Engineering Characteristics of Peaty Clay using Wet Cement Mixing Method

D.S.R.C.V. Perera
Department of Civil and Environmental Engineering, University of Ruhuna

ABSTRACT: With the developments, the geotechnical engineers have to be compelled with erecting structures on a variety of subsoil conditions varying from the most desired to the worst founding soil *i.e.* peaty clay in Sri Lankan context. Some prominent projects in Sri Lanka are facing the issue of peat being the thick founding soil on which to build new structures. Construction on peaty clay leads to substantial problems during the construction and long-term settlements during the service due to its very low shear strength and very high compressibility. Even disposal of peat and refilling with fair soil, despite the fact that inadmissible environmental impacts can occur, is also being practiced as a remedy to the current problem. Preloading efforts have also been practiced which have yielded long-term strength gain pattern owing to lengthier less intense loading, for soil having low shear strength avoiding sustaining a higher load once. Thus accelerated workflow is inhibited. The cement mixing strategy is one of the most environmentally friendly and economically feasible ground improvement techniques which is acknowledged around the world. The sui generis purpose of the strategy is to enhance sub-soil characteristics by in-situ mixing the soil with cement and other binders replacing cement to optimize the cost. In this research, the effect of wet cement mixing on improvement of strength and compressibility of peaty clay were assessed.

1 INTRODUCTION

Nowadays, infrastructures have been dramatically increased in the developing countries. In Sri Lanka, most of the infrastructure development projects, such as expressway constructions are ongoing at locations where there are soft soils with substantial thickness. For example, Southern Expressway Extension Projectand Outer Circular Expressway Project are going through an area underlain with very soft peaty clays. Peaty clay gives rise to enormous geotechnical engineering problems due to its high water content, very low shear strength and very high compressibility. As such, peaty clay does not provide favourable conditions for construction on them. Therefore, Geotechnical Engineers face challenges in the construction of expressways through sites underlain with thick layers of peaty clay.

Improvement of existing soft soil to an adequate level and use of deep foundations to transfer the loads to an underlying competent soil layer are the two options available. With the developments of roads that occupy a large plan area, improvement of the in-situ ground condition becomes the more viable option.

The deep mixing method is a world-wide accepted ground improvement technology at present (Souliman, 2011).The unique purpose of this method is to improvestrength parameters of soft soil by in-situ mixing with cement and other additives.

Although deep mixing technique has been successfully utilized to improve soft soil in other countries such as Japan and Sweden for more than 2 decades, it has been adopted in Sri Lanka to improve soft peaty clay in very recently (Saputhantiri and Kulathilaka, 2011).Even though, in Sri Lanka, many researchers have done laboratory scale studies on cement mixing technique, nowhere in the country has adopted this technique in the field for stabilizing soft organic clay or soft inorganic clay. In some of the recent infrastructure development projects in Sri Lanka, cement mixing technique has been proposed to improve the soft soil at the initial stage, however it has not been implemented due to many reasons, such as; not sufficient shear strength gain after mixing soft soil with cement at the laboratory scale tests and technical issues related to soil-cement mixing in the field.As such, remove and replacement method has been adopted instead of deep mixing technique without considering the environmental effect.

Cement mixing is considered as one of the most efficient and economical methods to improve soft soil, even though it is not yet successful implemented in Sri Lanka. Hence, in this research study, attempt has made to improve the engineering characteristics of soft peaty clay mixing with cement and other industrial by-products such as Rice Husk Ash (RHA).

2 METHODOLOGY

2.1 *Material*

Soft peaty clay samples were collected fromNilwala flood plain where Southern Expressway Extension Project is going on. Since deep mixing technique was rejected in this project without conducting any comprehensive study, applicability of the deep mixing technique for above ground condition was studied under this research. Basic properties of the peaty clayare illustrated in Table 1.

Table 1. Basic properties of peaty clay

Property	Value
Natural moisture content	177 %
Bulk unit weight	11.38 N/m^3
Specific gravity (Gs)	2.03
Organic content	23 %
Liquid Limit (LL)	155 %
Plastic Limit (PL)	61 %
Plastic Index (PI)	94 %
Linear shrinkage	8 %
pH value	5.3
Void ratio(e_0)	4.56
Compression Index (C_c)	1.57
Modified Compression Index C_c')	0.28
Swelling Index (C_s)	0.06
Undrained shear strength (C_u)	12.0 kN/m^2

Commercially available Ordinary Portland Cement (OPC) was used as the main binding material and Rice Husk Ash (RHA) was used as the pozzolanic additive. RHA was collected from Brick kiln at Tissamaharama area.

2.2 *Sample preparation*

Remouldedpeaty clay samples were used for the laboratory test. Prior to each test, large debris, undecayed pieces of wood, gravel particles and unwanted particles were removed. After remoulding, peaty clay were kept in a water bath for few days to make sure that soil is fully saturated. With the objective of improving the engineering characteristics soft soil, soft peaty clay were mixed with cement slurry and RHA at different mix proportions as shown in Table 2. Sample prepared by mixing nine parts of peaty clay (90 %) with one part of cement (10 %) on weight is designated as PC10. In similar lines, in samples PC20 and PC30, cement content was 20 and 30 % respectively. Unimproved peaty clay is represented as PC0. Sample prepared by mixing eight parts of peaty clay (80 %) with one part of cement (10 %) and one part of RHA (10%) on weight is designated as PC10RHA10.

Peat was obtained from Nilwala flood plain where expressway projects are underway. RHA was collected from domestic brick kilns in Thissamaharama area. Initial basic propertiesWet cement slurry was prepared by keeping a water to cement ratio of 0.3. Mix proportions were selected on weight basis and in order to ensure uniform level of mixing, allsamples were mixed in the concrete mixer at same rotation speed of 60 revolutions per minute for a period of 10 minutes.For each mix proportion, 5 test cubes, which are 150 mm x 150 mm x 150 mm dimensions, were casted. After 24 hours, steel moulds were removed and soil-cement blocks were submerged in a water bath for curing to simulate the field condition. One test cube from each mix proportion was tested for compressive strength after 14 days where as 3 test cubes were tested after 28 days to evaluate the short term stabilization. The remaining test cube was tested after 100 days to evaluate the long term stabilization.

Oedometer samples with diameter of 50 mm and thickness of 20 mm were prepared for each mix proportion and these specimens were kept under submerged conditions for 28 days. Then oedometer tests were conducted for each specimen to find the improvements in the compressibility characteristics.

3 RESULTS AND DISCUSSION

3.1 *Effect of cement on strength improvement*

The unconfined compressive strength of improved peaty clay is illustrated in Table 2. Figure 1 clearly illustrated that unconfined compressive strength of soft peaty clay is significantly increased with the increase of cement content. Effect of curing period on strength gain is also illustrated in the same figure. Similar to the concrete, it can be clearly seen that strength gain of soil-cement mixtures after 14 days is about 70% of that of 28 days strength. Further, it can be noted that unlike the strength gain trend of concrete, cement slurry treated peaty clay exhibit the effect of long term curing, where there is a considerable strength gain after 100 days. In longer duration, much time is available for C_a^{2+}irons in the cement to get attached with soil particles and to occur flocculation and thereafter the pozzolanic reaction. This implies, cement hydration and pozzolanic reaction occur for a long period of time after mixing, as such strength of cement treated peaty clay is increased with time. Note that by mixing 10% of cement with peaty clay, 28 days unconfined compressive strength could be increased to about 1 MPa.

3.2 *Effect of RHA on strength improvement*

The variation of unconfined compressive strength of peaty clay improved with 10% cementover Rice

Husk Ash (RHS) is shown in Figure 2. Based on the results, it can be seen that unconfined compressive strength gradually increases with the addition of RHA. Due to presence of about 88% of SiO_2 within the RHA enhance the development of secondary cementitious product. However, when the RHA content is more than 20%, unconfined compressive strength is drastically decreased irrespective of the curing period. Addition of RHA by replacing cement may cause to reduce the Ca^{2+} iron content within the peat-cement mixture. As such, even though SiO_2 increases with the addition of RHA, the secondary cementitious product will not develop, resulting low strength. Similar behaviour can be observed with higher cement percentages on peat-cement mixtures. Hence, it can be concluded that addition of 10% cement together with 20% RHA is effective in increasing the 28 days unconfined compressive strength of peaty clay to more than 2 MPa.

Table 2. Strength of improved peaty clay

	Unconfined compressive strength q_u(MPa)		
	After 14 days	After 28 days	After 100 days
PC0		C_u=12 kPa	
PC10	0.71	0.97	1.14
PC20	2.42	3.43	4.40
PC30	5.45	6.76	7.11
PC10-RHA10	2.04	2.73	3.25
PC10-RHA20	2.23	3.37	4.64
PC10-RHA30	0.73	1.47	1.57
PC20-RHA10	5.60	7.13	7.89
PC20-RHA20	3.15	5.76	7.77
PC20-RHA30	1.31	1.37	1.47
PC30-RHA10	13.80	15.57	22.9
PC30-RHA20	17.18	21.59	25.37
PC30-RHA30	5.31	6.40	7.16

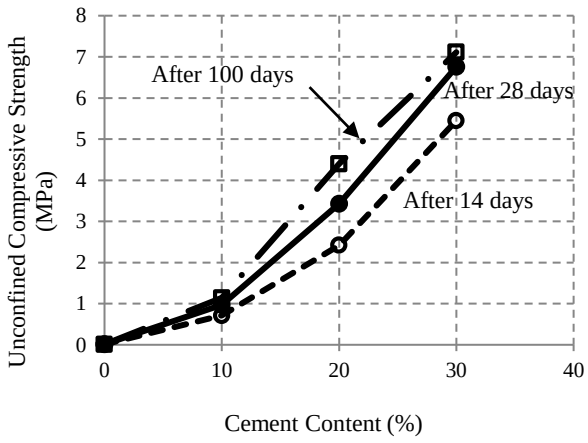

Fig. 1Effect of cement on unconfined compressive strength

3.3 *Variation of e Vs Log (σ_v') relationship*

Variations of primary consolidation characteristics were illustrated through *e* vs log (σ_v') plot and results are summarized in Table 3. The typical plots for 10% cement treated peaty clay together with RHA are presented in Figure 3. It can be clearly seen that initial void ratio significant reduced with the addition of cement. The combine use of cement and RHA can further reduce the initial void ratio. Similar to the strength behaviour, when the RHA content is more than 20%, initial void ratio has been increased.

It can be observed that modified compression index {$C_c/(1+e_0)$} significantly decreased with the cement content. Just adding 10% of cement, modified compression index could be reduced by an order. A noticeable reduction in modified compression index could be achieved by combining RHA with cement.

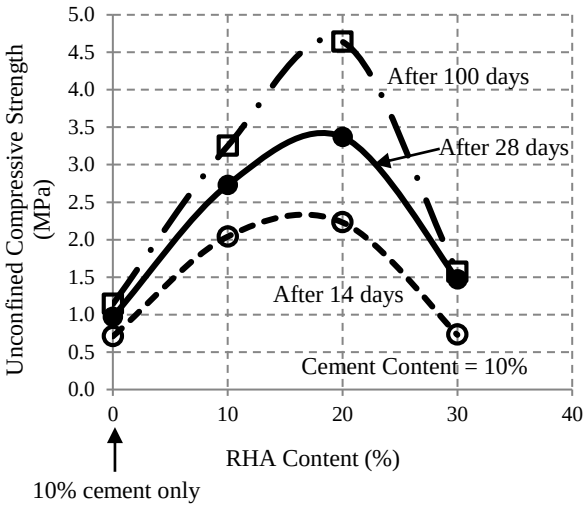

Fig. 2Effect of RHA on unconfined compressive strength

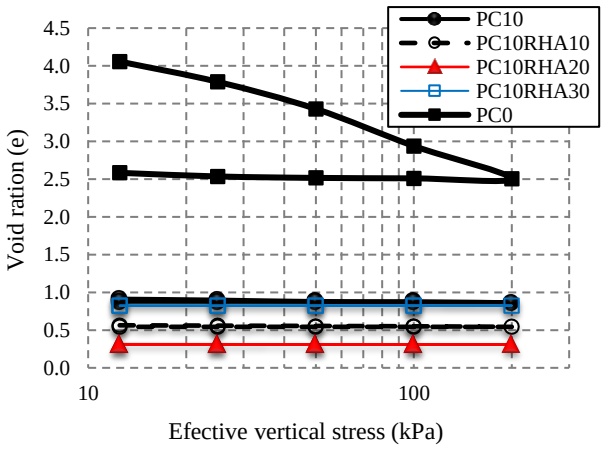

Fig. 3*e* vs log (σ_v') relationship for 10% cement treated peaty clay

3.4 *Variation of coefficient of volume compressibility*

Coefficient of volume compressibility (m_v) can be considered as an alternative parameter for estimating settlement. It was evaluated at each and every stress level. The influence of cement and RHA on m_v is illustrated in Figure 4. The figure clearly illustrated that $m_v$values were drastically reduced when the peaty clay mixed with cement. m_v value has been further reduced with the addition of RHA.

Table 3. Consolidation characteristics

	e_0	C_c	$C_c/(1+e_0)$
PC0	4.560	1.5700	0.2820
PC10	0.922	0.0532	0.0277
PC20	0.756	0.0199	0.0113
PC30	0.411	0.0099	0.0070
PC10-RHA10	0.565	0.0149	0.0095
PC10-RHA20	0.322	0.0066	0.0050
PC10-RHA30	0.836	0	0
PC20-RHA10	0.431	0.0099	0.0069
PC20-RHA20	0.320	0.0150	0.0114
PC20-RHA30	0.442	0	0
PC30-RHA10	0.121	0.0033	0.0029
PC30-RHA20	0.236	0.0121	0.0098
PC30-RHA30	0.353	0.0033	0.0024

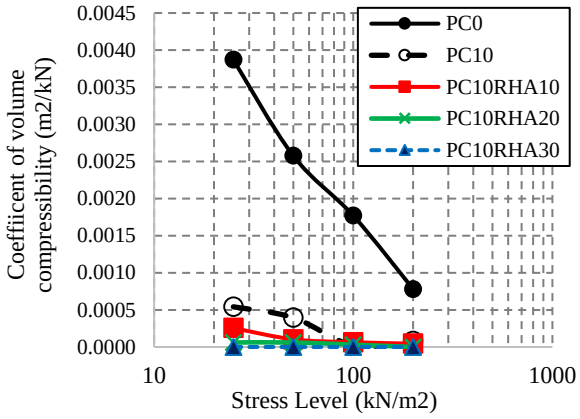

Fig. 4Variation of m_v with stress level

3.5 *Scanning Electron Microscope (SEM) Analysis*

The behaviour of unconfined compressive strength and compressibility characteristics over varying cement and RHA contents could be justified by the Scanning Electron Microscope (SEM) observations where material interlock and bond structure were the key parameters. Figure 5 shows the SEM images of untreated and treated peaty clay. The irregular shapes of the peaty clay particles together with voids are shown in Figure 5(a). Particles have been changed to more flocculated structure after mixing 10% of cement with peaty clay as depicted in Figure 5(b). Irregular shapes of the peaty clay have been changed to slightly barshapes due to formation of secondary cementitious material. This behaviour has been further improved after mixing with RHA as shown in Figure 5(c).

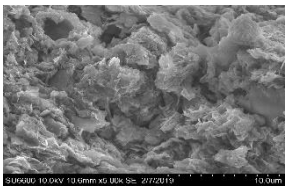

(a) PC0

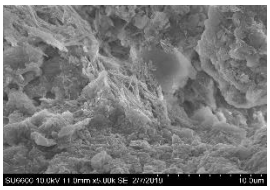

(b) PC10

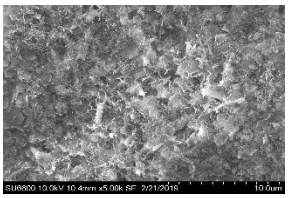

(c) PC10RHA10

Fig. 5Change of microstructure

4 CONCLUSIONS

Wet deep mixing provides higher improvements in terms of both unconfined compressive strength and compressibility. 28 days unconfined compressive strength of cement treated peaty claywas more than 3 MPa when the cement content is more than 20%. However, the usage of high amounts of cement as the sole stabilizing agent for wet deep mixing is not cost effective. Considerable improvements could be extracted from 10% of cement with added 10% RHA despite the fact it was less than that of the 20 % cement mixes. 100 days unconfined compressive strength illustrated that cement hydration and pozzolanic reaction can last for long period of time after mixing. Compressibility characteristics of peaty clay were significantly improved by mixing with cement. By adding RHA to peat-cement mixes, compressibility characteristics could be further reduced. Thus it could be concluded that 10% of wet cement slurry together with 10% of RHA would be the ideal combinationto improve soft peaty clay with respect to both economy and structural fit.

REFERENCES

Saputhantiri D.R andKulathilaka S.A.S (2011), Enhancement of Engineering Characteristics of Peaty Clay due to Mixing With Cement, Annual Transactions of Institute of Engineers Sri Lanka. pp 118-126.

Souliman, M. (2011). International Case Studies of Peat Stabilization by Deep Mixing Method, Jordan Journal of Civil Engineering. - Vol. 5, No. 3, pp. 424-430. Irbid: Jordan University of Science and Technology.

Comparison of Different Philosophies on Design of Load Transfer Platform of Piled Embankment

M.H.A.N.P.S. Perera and N.H. Priyankara
Department of Civil Engineering, University of Ruhuna, Sri Lanka

ABSTRACT: Geotechnical engineers face different challenges when designing structures including highway embankment over soft, compressible soil or weak foundation soil, which resulted in many issues, including intolerable settlements, potential bearing failures, large lateral pressures and movements and global and local instability. There are different ground improvement methods available such as wick drains, surcharge loading, vibro concrete column and etc. But piled embankment is an economical and efficient load transfer method which can be achieved using geo-synthetic reinforcement material. Results of parametric study to investigate the applicability of finite element method for analyzing different philosophies to design of load transfer platform of piled embankment in this paper. Results reveal that use of load transfer platform and pile cap can decrease the failures. Significant reduction of settlements and bending moment by using an inclined pile or geo-synthetic. BS method is most effective and economical solution than Collin's method.

1 INTRODUCTION

The major properties of soft soil are much compressibility, low shear strength, lacking bearing capacity and a propensity to long-term consolidation settlement. As a result of these properties, embankments built on soft soil be apt to deform after many years after the construction. Modern soil improvement techniques involve the use of geo-synthetics.Layers of geo-synthetic reinforcement which platform is called as "Load Transfer Platform". It enhances the load transfer mechanism and considerably minimize the differential and maximum settlement. This load-transfer platform, located between the embankment and the piles, is a compound of the granular material compacted between a number of horizontal layers of high-strength geo-synthetics. In the load-transfer platform, the geo-synthetics have three functions. They increase the pressure on the piles, restrict and annul the lateral spreading at the embankment edge, and separate the embankment from the foundation soil. (Kaluder et al., 2015)

In Matara - Hambanthota Expressway development (Southern Expressway Extension project), piled embankment with spun piles were suggested as the ground improvement technique in Godagama Interchange area.

There are analytical and numerical methods to analyze such a platform according to the different standards. Numerical methods such as finite element analysis are available for analyze complex soil-interaction problems. In this paper investigate the most effective method to design load transfer platform of piled embankment by using Plaxis-2d software by observing different parameters. A clear technical and economic assessment of different philosophies available to design load transfer platform.

2 METHODOLOGY

This research is focused to analyze and compare the behavior of piled embankment design. The Finite Element Method, Plaxis 2D modelling which is appropriate to simulate the behaviour of the pile embankment system in complex engineering problems. Plaxis software is the one of the most reliable, user friendly software.

The basic properties of soil, geo-grid and pile have to be identified as input data to the software. Required input data have been acquired from borehole investigation reports, soil test reports and relevant local findings. Sub surface soil profile have been identified by using borehole test data as shown in Figure 1.

Some boundary conditions have been considered:

- Both vertical sides are pinned and base is fixed supported
- Pavement and traffic load (25 kN/m^2)

Initial condition – It is assumed that thickness of 1membankment fill platform will be placed on the unimproved soft soil ground and piles will be installed at relevant spacing with or without pile cap, and thickness of 1.2m load transfer platform (ABC material) will be constructed together with relevant numbers of geotextile.

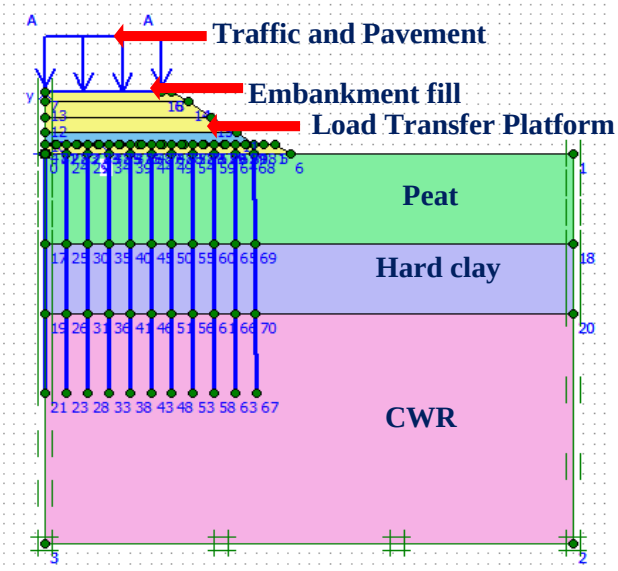

Figure 1: Sub surface soil profile

After the geometry modal completed, finite element model (mesh) have been generated. After mesh generated, initial conditions have been generated which comprise initial porewater pressure condition, the initial effective stress condition and etc. Then phases of construction procedure was used for simulation of the realistic process of piled embankment construction as follow.

Phase 1 - Embankment 1st layer construction (1.5 m height)
Phase 2 - Consolidation of 1st layer for 21 days
Phase 3 - Embankment second layer construction (1.5 m height)
Phase 4 - Consolidation of embankment (2nd layer) for 21 days
Phase 5 - Embankment third layer construction (1 m height)
Phase 6 - Consolidation of embankment (3rd layer) for 14 days
Phase 7 - Consolidation period until open to traffic (300 days) with only pavement load
Phase 8 - Road open to traffic
Phase 9 - Road open to traffic after 3 years (1095 days)

Vertical settlement and lateral displacement of the embankment and bending moment and axial forces of each piles have been analyzed after 3 years consolidation(road open to the traffic)by varying variables such as pile spacing, pile cap size, embankment fill height and number of geo-synthetic layers and its strength class using numerical modelling

3 RESULTS AND DISCUSSION

When considering embankment with only pile without pile cap, Load Transfer Platform and geotextile, there are some failures occurs at the top of the embankment, Vertical deformation of outside of the embankment, horizontal deformation and maximum bending moment of piles as shown in figure 2. There is nosignificant vertical settlement of within the embankment. Therefore only vertical settlement of outside the embankment has been considered.

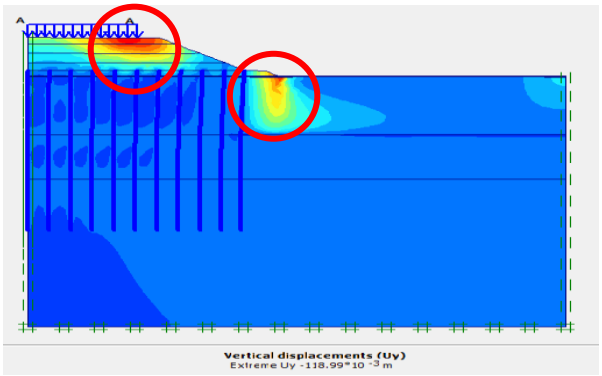

Figure 2: Vertical displacement of soil profile

When considering results with the Load Transfer Platform, all the parameters such as bending moment, horizontal deformation, vertical deformation is reduced with the load transfer platform. There is a load transference due to load transfer platform which consists of gravel material. So results have been analyzed further with the load transfer platform.

3.1 *Treatment for failures*

There is a significant reduction of Horizontal deformation and Vertical deformation of embankment and maximum bending moment of pile when applying an inclined pile and geotextile as shown in Figure 3 and Figure 4 respectively.

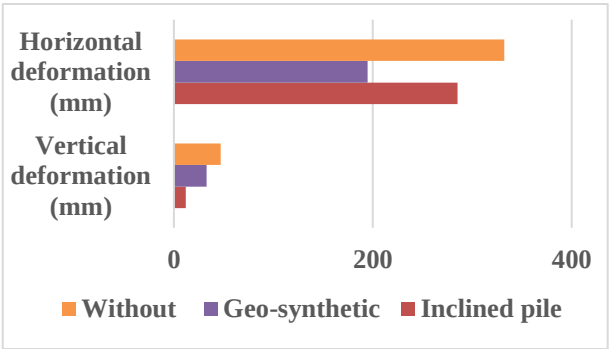

Figure 3: Horizontal and Vertical deformation varying with geo-synthetic and inclined pile

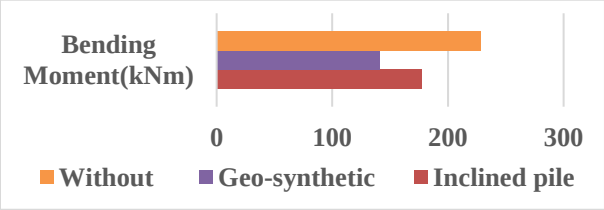

Figure 4: Bending moment varying with geo-synthetic and inclined pile

3.2 *Axial force variation with geo-synthetic*

In this model, piled embankment with different pile cap sizes is considered and axial force variation has been analyzed with the geo-synthetic behavior. Due to membrane action of the reinforcement, the load transfer mechanism can be identified by referring variation of the axial force as shown in figure 5.

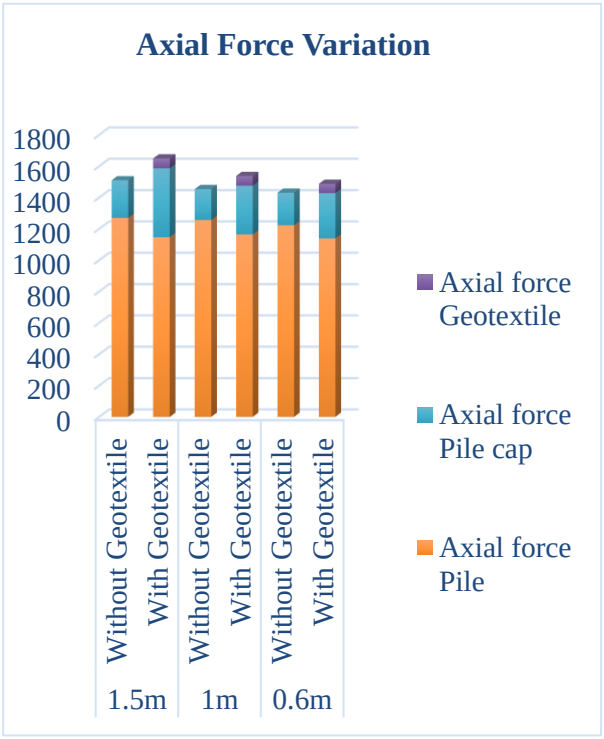

Figure 5: Axial force variation with pile cap size

Load transfer mechanism of the geo-synthetic reinforcement will decrease the parameters due to large amount of load transfer to pile and pile cap by geo-synthetic.

3.3 *Comparison of different philosophies*

BS method says it is better to use one geotextile for load transfer platform and Collin's method says three geotextile much better than one geotextile. Parametric study have been done for both methods considering 600/50 strength 1 geotextile and 200/50 strength 3 geotextiles. There is no much difference of vertical and horizontal deformations with the variation of pile spacing, pile cap size and fill height as shown in Figure 6, Figure 7 and Figure 8.

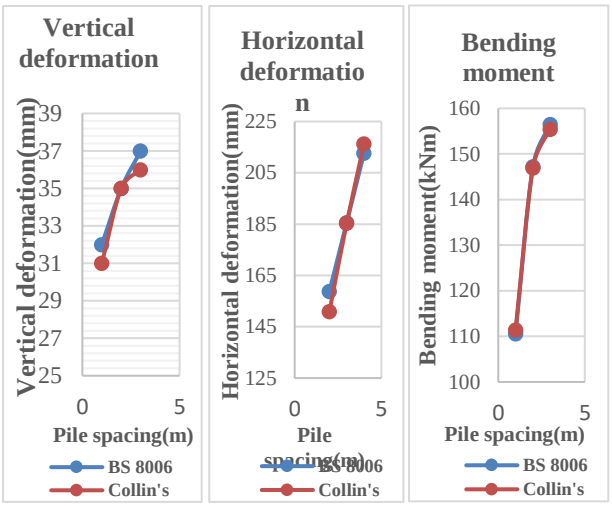

Figure 6: Parameter variation with pile spacing for different philosophies

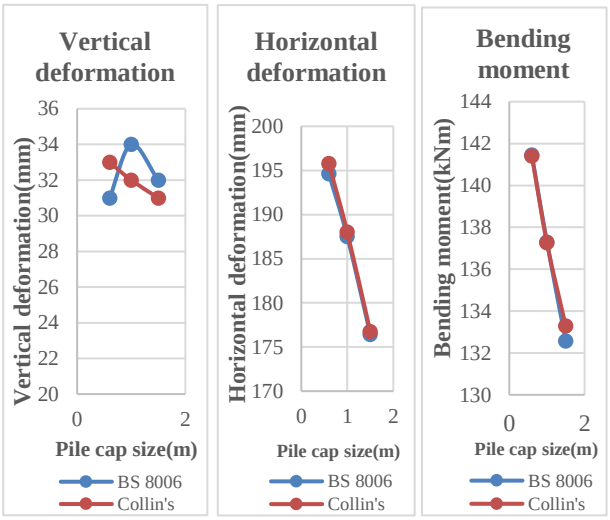

Figure 7: Parameter variation with pile cap size for different philosophies

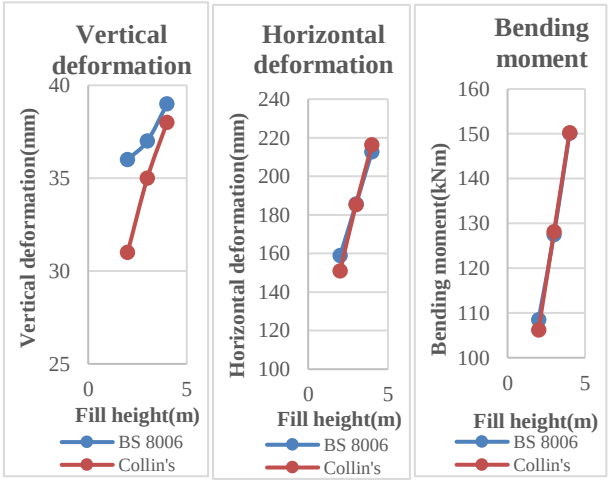

Figure 8: Parameter variation with embankment fill height for different philosophies

According to the results BS method and Collin's method gives slightly similar results for different parameters. When considering economical comparison, 200/50 and 600/50 strength geotextile per square meter is about Rs.1400/- and Rs.1900/- respectively. Therefore considering both analysis, BS method is most suitable method to design load transfer platform of piled embankment.

4 CONCLUSION

Based on the numerical modelling results Collins method and conventional BS method gives similar results. It is better to conclude with economic analysis. Considering both analysis BS method is most suitable method to design load transfer platform. But Collin's method is most suitable when the critical parameter is vertical settlement.

It is observed that when the pile spacing is decreasing settlement, horizontal deformation of the embankment and maximum bending moment of the pile also decreasing. When the pile cap size is increasing, all parameters will decreasing.

There is a significant reduction of horizontal and vertical settlement and bending moment when applying an inclined pile and geotextile.

As per recommendation conclusion can be proceed for the actual situation with the validation of the model.

REFERENCES

Collin, J.G., Han, J., and Huang, J. (2005), "Design Recommendations for Column Supported Embankments," FHWA-HRT, August.

Fei, K., 2014. *A Simplified Method for Analysis of Geo- synthetic Reinforcement Used in Pile Supported Embankments.* China, Hindawi Publishing Corporation

Gangakhedkar, R., 2004. Geo-synthetic Reinforced Pile Supported Embankments, Master thesis, University of Florida.

Gangatharan, R., 2014. *Comparison between piled embankment and load transfer platform – rigid inclusion for soft soil,* Florida.

Han, J. and Gabr, M.A., (2002*). A numerical study of load transfer mechanisms in geo-synthetic reinforced and pile supported embankmentsover soft soil. Journal of Geotechnical and Geoenvironmental Engineering,* ASCE, 128(1), pp. 44-53

Kaluder, J., Mulabdic, M. &Minazek, K., 2015,"Comparison of design methods", Load Transfer Platform, October, University of Osijek, Faculty of Civil Engineering Osijek, pp.30-40.

Nanayakkara N.G.G.S.D., 2017. *Numerical analysis of spun concrete piled embankment,* University of Ruhuna.

The Effect of Grouting Pressure on Pullout Resistance of Soil Nails

R.G.F. Harshini

Department of Civil and Environmental Engineering, University of Ruhuna, Sri Lanka

ABSTRACT: Soil nailing is an in-situ reinforcement technique that has been increasingly used in slopes, especially cut slopes, to improve the stability of slopes. Advantages such as short construction period and low cost are the main reasons for its increasing popularity. Furthermore, it is very suitable for stabilizing slopes in congested areas where access of heavy equipment is a problem. The pullout resistance of soil-nail is an important factor in design. The pullout resistance of soil-nail is mainly influenced by the soil–nail interface shear strength. Experience and previous research have shown that grouting pressure increases the soil–nail interface shear strength. It is common practice with soil-nail construction to adopt gravity or low pressure grouting. The use of grouting pressure is an effective way of increasing the soil nail pullout resistance. However, the mechanism of how the grouting pressure influence the pullout resistance of soil-nails are not well understood. As such, in this research study, laboratory scale model setup was used to study the effect of grouting pressure on pullout resistance.

1 INTRODUCTION

Soil nailing technique has been most commonly used as slope stabilizing method especially for cut slopes and retaining structures from last two decades (Hong et al., 2013). Further, it is very suitable for stabilizing slopes in congested areas where access of heavy equipment is a problem.

For design of a soil-nail system, the interface shear strength between soil-nail and the surrounding soil is a key factor for the design. The soil-nail interface shear strength is normally verified by pullout tests in the construction stage (Yin et al., 2009). However, pullout resistance of a soil-nail system is difficult to estimate with high accuracy due to many uncertainties in the field. Many factors have been influencing the soil–nail interface shear strength. According Pradhanet al., 2006, grouting pressure is a key factor on soil–nail interface shear strength. Usually, during the soil-nail construction, gravity or lowpressure groutingis adopted. Use of high grouting pressure on soil-nail system is an effective way of increasing the pullout resistance (Pradhan et al., 2006). However, the mechanism of how the grouting pressure influence the pullout resistance of soil-nailsystemis not well understood yet.As such, in this research study, laboratory scale model setup was used to study the effect of grouting pressure on soil-nail pullout resistance.

2 METHODOLOGY

2.1 *Material*

Commonly available lateritic soil was used as the test material in this research study. The basic properties of the soil are depicted in Table 1. According to Unified Soil Classification System (USCS). soil type was classified as well graded sand (SW).

Table 1Physical properties of Lateritic soil

Property	Value
Liquid Limit (%)	58
Plasticity Index (%)	28
Optimum Moisture Content (%)	17.53
Maximum Dry Unit Weight (kN/m^3)	17.0
Specific Gravity (G_s)	2.39
Coefficient of Uniformity (C_u)	6.39
Coefficient of Curvature (C_c)	1.09

2.2 *Laboratory model setup*

Figure 1 illustrates the basic instrument arrangement of laboratory model setup, which encompass portal frame, pullout box and grouting cylinder. The internal dimension of the pullout box is 600mm (length) × 460mm (width) × 600mm (height). A lubricant was appliedon internal faces of the steel box to reduce the friction between steel box wall and soil.

An additional chamber with dimensions of 280mm in length × 130mm in width × 130mm in height was connected to the end of the steel box. Chamber was filled with same compacted soil in the box. A hole was drilled from front of the box to 250mm into additional chamber. Afterward, a nail was inserted into the hole with centralizers and grouted with cement slurry. After curing, soil in the chamber was removed. Therefore, during the pullout test, grouted nail can be pullout up to 250mm of horizontal displacement with having full contact with soil.

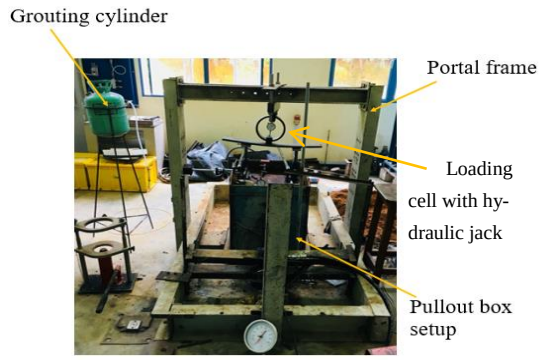

Fig. 1 Laboratory setup

Grouting cylinder has three valves namely grout inlet, grout outlet and inlet valve for compressed air. Compressed air was driven through the cylinder and which was controlled through a valve.

2.3 *Laboratory test procedure*

The soil was compacted into steel box with 90% of maximum dry unit weight. The soil was filled with compacted layers, which have a thickness of 50mm. Five Earth Pressure Sensors (EPS) were installed at 3 different depths within the soil. 3 numbers of EPS were installed 40 mm above the nail surface at near the nail head, middle and tail. Other 2 EPS were installed 100mm away from bottom and top surface of the steel box. Cross section of the laboratory model setup together with instrumentations is shown in Figure 2.

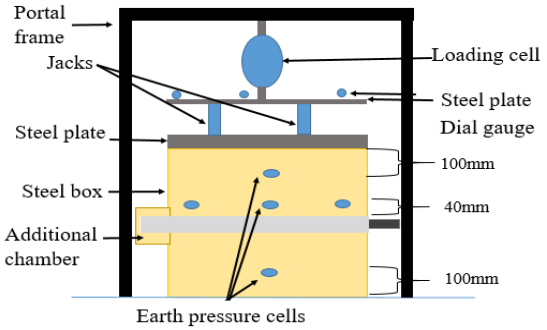

Fig. 2 Cross section of laboratory model setup

Surcharge loadwas applied by jacking two hydraulic jacks fixed to a portal frame and monitored by a load cell.Once the EPS readings were reached to a constant value, after 24 hours from the application of overburden pressure, a horizontal hole was drilled using a hand auger from front of the steel box. Then 10mm diameter steel bar was installed into the predrilled hole with centralizers. The hole was grouted with specified grouting pressure for each test. Four numbers of model tests were conducted with varying the grouting pressure from 40kPa to 100 kPa at intervals of 20 kPa. Water/Cement ratio of cement grout was kept as 0.5 (Pradhan et al., 2006). Non-shrinkageadmixture was mixed with cement slurry to increase the harden period.

According to Yin et al., 2009, cement slurry could gain sufficient strength after 5 days of curing. Then pullout test was conductedusing a hydraulic jack and pullout force readings were noted together with horizontal displacement manually. Throughout the test, EPS readings were recordedusing a computer control data acquisition system.

2.4 *Numerical Analysis*

Numerical modeling was done using *PLAXIS-2D*software in order to simulate the conditions of the laboratory model setup for a soil-nail interface to obtain the pullout resistance numerically. The input geometry of the model is shown in Figure 3. A prescribed overburden pressure was assigned to the input geometry. Grouting pressure was simulated by applying a surcharge load, which is equivalent to the grouting pressure, surrounding the soil–nail system. Pullout forces were obtained by applying prescribed displacements to the nail head. Horizontal displacements were varied up to 60 mm at 5 mm interval and the frictional stresses developed at the soil-nail interface were resulted from the model analysis. The analysis was done in staged construction mode and the stresses at each phase were resulted from the analysis.

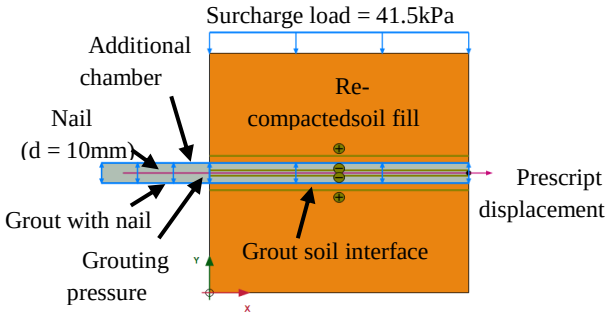

Fig. 3 Input geometry of PLAXIS-2D model

3 RESULTS AND DISCUSSION

3.1 *Variation of earth pressure during the soil-nail installation*

Change of earth pressure during the application of overburden pressure of 40 kPais depicted in Figure 4. Soon after the application of the surcharge, earth pressures indicate slightly higher overburden pressure than the actual due to movement of the soil particles in contact with EPS. After 16 hours, there is no any changes in the measured earth pressures indicating that the vertical stress of the soil has

been reached to constant and reflected the applied overburden pressure.

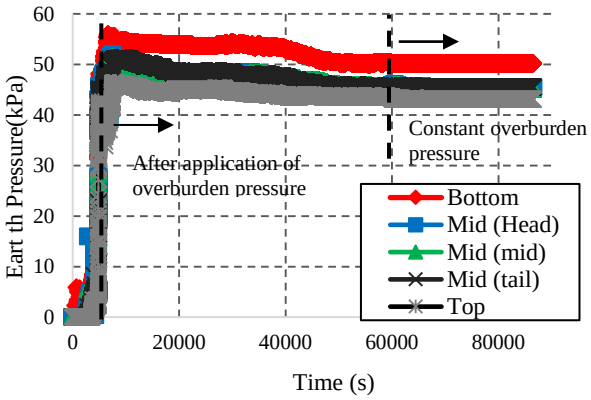

Fig. 4 Variation of earth pressure due to application of overburden pressure

During the drilling for nail installation, vertical pressure is reduced due to stress release in surrounding soil. As such, normal stress on the nail may vary during the installation indicating the importance of simulation of stress release and examination of earth pressure variations. This behaviouris clearly illustrated in the Figure 5. From the figure, it can be observed that earth pressure has been slightly increased due to outward movement of the soil particles during the drilling operation. Once the drilling tool had passed the location of the EPS, earth pressure has been reduced due to release of stress. Further, it can be noted that earth pressure has reached to slightly equilibrium condition before apply the grouting pressure. A rapid increase of earth pressure could be observed at middle EPS at about 1100 second owing to the action of pressure grouting. The pressure increase was lasted for about 8 minutes and then pressure has been reduced and reached to equilibrium; this value is approximately equal to the pressure before grouting. This pressure reduction was due to hardening effect of cement grout.

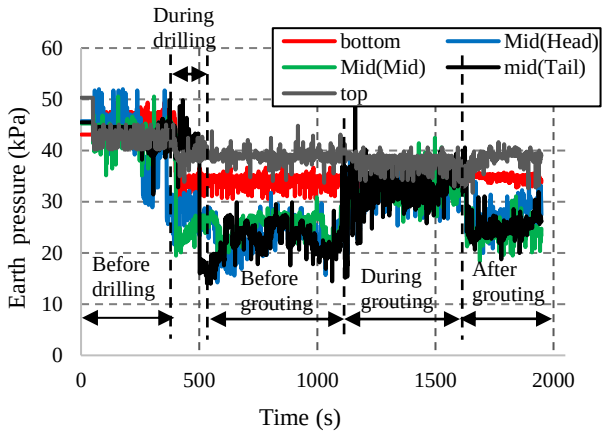

Fig. 5 Variation of earth pressure during nail installation

3.2 *Pullout resistance*

Figure 6 illustrates the measured pullout force plotted against nail head displacement under an overburden pressure of 40kPa and grouting pressure of 40kPa, 60kPa, 80kPa and 100kPa.It can be seen that pullout force increases with the grouting pressure. During the drilling of a hole to install nail, surrounding soil of the hole is loosened and soil-arching effect developed to retain the soil above the hole. During the pressurized grouting, the hole is compacted with cement slurry. Further, cement grout has been penetrated into the voids of loosened soil particles around the drill hole and solidify the soil particles, resulting increase the bond strength.The higher the grouting pressure, greater the increase in bond strength. This could be further verified by inspecting the grouted nail diameter after the test as presented in Table 2.Even though, predrilled hole diameter is 50 mm, with the grouting pressure, grouted nail diameter is more than 50mm. Greater the grouting pressure, larger the grouted nail diameter. As such, pullout resistance increases with grouting pressure.

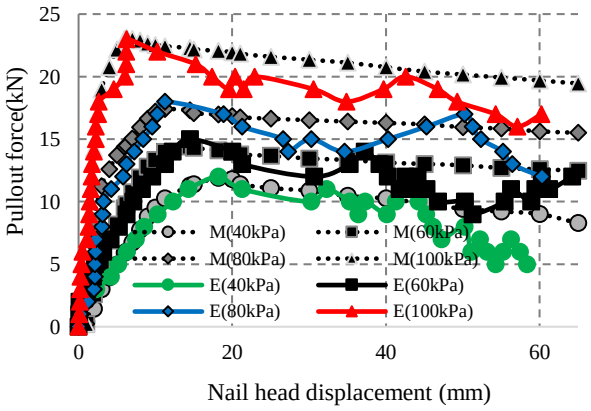

Fig. 6Variation of pullout force over nail head displacement

Table 2.Grouted nail diameter over grouting pressure

Grout pressure(kPa)	Grouted nail diameter (mm)
40	54.94
60	57.06
80	59.60
100	62.90

The earth pressure variation during pullout test is shown in Figure 7. There is no any variation of earth pressure away from the nail (nails at top and bottom) indicating that effect of pulling of nail to the surrounding soil is localized. It can be seen that earth pressure close to nail head had increased to highest value at peak pullout force. The pressure response of EPS at middle and tail of the nail were delayed when compared with that of EPS at nail

head. This is a clear indication that gradual transfer of stresses from soil to the nail.

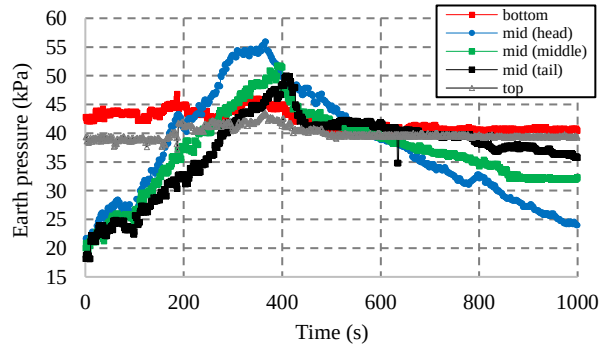

Fig. 7 Variation earth pressure during pullout test

3.3 *Comparison of experimental results with numerical results*

The comparison of the experimental results and numerical results over grouting pressure is shown in Fig.6. It can be noted that numericalresults are well agreed with the experimental results. The comparison of peak pullout forces on experimental and numerical analysis is illustrated in Figure 8. It is very clear that peak pullout forces determined based on both methods are almost same indicating the accuracy of the parameters adopted for the numerical modeling.

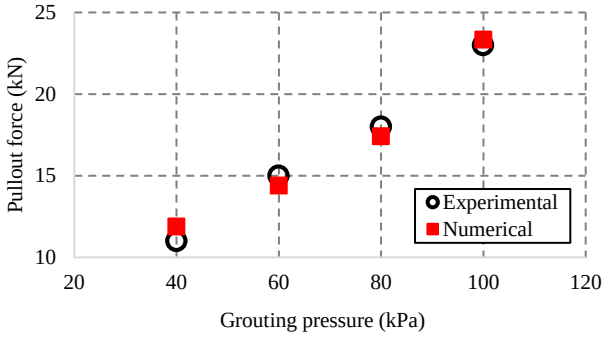

Fig. 8 Comparison of peak pullout results

The development higher earth pressure close to the nail head during pullout test is associated with the greater shear displacement. This behaviourcould be clearly illustrated numerically as shown in Figure 9, where greater shear stress has been developed near the nail head. As such, greater shear displacement has been occured close to the nail head resulting higher earth pressure.

Fig. 9 Variation of shear stress along the nail during pullout

4 CONCLUSIONS

Laboratory experimental study as well as numerical study has been carried out to study the effect of grouting pressure on pullout resistance. Based on the research study following conclusions can be made.

- The earth pressure surrounding hole has been dropped during the drilling to place nail due to release of stress.
- By increasing the grouting pressure, pullout resistance could be significantly increased.
- Grouted nail diameter was increased with the grouting pressure, resulting greater bond strength between soil and nail.
- Greater earth pressure was develop close to the nail head than that of tail during pullout of nail due to development of higher shear displacement close to the nail head.
- The stresses of soil were gradually transferred to nail starting from nail head to the nail tail during the pullout of nail.

REFERENCES

Hong, C.Y., Yin, J.H., Pei, H.F. and Zhou, W.H., 2013. Experimental study on the pullout resistance of pressure-grouted soil nails in the field, Canadian geotechnical journal, 50(7), pp.693-704.

Pradhan, B., Tham, L.G., Yue, Z.Q., Junaideen, S.M. and Lee, C.F., 2006. Soil–nail pullout interaction in loose fill materials, International Journal of Geomechanics, 6(4), pp.238-247.

Yin, J.H., Su, L.J., Cheung, R.W.M., Shiu, Y.K. and Tang, C., 2009. The influence of grouting pressure on the pullout resistance of soil nails in compacted completely decomposed granite fill, Geotechnique, 59(2), pp.103-113.

Influence of Type of Interfaces on Railway Ballast Behaviour

K.R.C.M. Gunawardhana, M.A.S.P. Gunawardhana and S.K. Navaratnarajah
Department of Civil Engineering, University of Peradeniya, Sri Lanka

ABSTRACT: Railroads are one of the most popular modes of transportation system. With the increase of congestion in road transport has created severe challenges to the sustainability of rail transport infrastructure. Due to the increase of speed and load, excessive lateral stresses are induced in rail track foundations. Ballast layer and various interfaces play significant role resisting lateral movement and give stability to track structures. Therefore,in this study the shear behavior of some interfaces in rail track were evaluated using large-scale direct shear apparatus considering full size ballast particles. The different interfaces studied in this research were wooden sleeper, concrete sleeper and Under Sleeper Pad (USP).Direct shear test of ballast particles was performed and that of different interfaces were compared.Maximum shear strength which occurred in ballast particle to particle interface and decreases accordingly ballast-concrete, ballast-timber and ballast-USP interfaces. Ballast degradation increases when normal load increases, and breakage decreases accordingly in ballast-concrete, ballast-timber and ballast-USP.

1 INTRODUCTION

Railway Ballast is the foundation of railway track and placed just below and around the sleepers. The loads from the wheels of trains ultimately come on to the ballast through rails and sleepers. The past studies have identified many functions of railway ballast.Suiker et al., (2005) have mentioned that the main function of ballast is to ensure fast drainage and reduce the magnitudes of vertical stress distributed to the underlying weak subgrade from heavy loading trains. According to Dahlberg, (2003) and Profillidis (2014) crushed, angular rock or hardstone ballast helps substructure to support against vertical, lateral and longitudinal forces from trains, provide firm and level bed for the sleepers to rest on; allow for maintaining correct track level without disturbing the rail road bed, discourage the growth of vegetation, protect the surface of formation and to form an elastic bed, hold the sleepers in position during the passage of trains; transmit and distribute the loads from the sleepers to the subgrade and provide lateral stability to the track as a whole. and also Abadi, et al., (2015) has proposed that by using, (a) finer ballast gradations, including the use of a layer of finer material beneath the sleeper (b) using softer USPs (c) using lower stiffness sleeper materials such as wooden or plastic sleepers, an increase in the number and area of contacts can be achieved in the sleeper to ballast interface.

In a railway track, wheel load is transferred through the different types of layers, first wheel load is taken by the rail then it is transferred to the sleepers after that it is transferred to the ballast then to the sub ballast and subgrade.Under Sleeper pads (USPs) and Under Ballast Mats (UBMs) both are called Shock Mats are used to improve the performance of rail track (Navaratnarajah & Indraratna, 2017 and Navaratnarajah et al. 2018). USP are installed between sleeper and ballast. UBM are installed between ballast and subgrade.There are many interfaces can be identified in rail track. Rail–Rail Pad, Rail Pad–Sleeper, Sleeper–Ballast, Ballast–Sub Ballast, Sub Ballast–Subgrade etc. Sleeper can be most commonly wooden, concrete or steel. If USP is used, Sleeper–USP and USP–Ballast interfaces can also be identified. Therefore, this study is to evaluate shear strength parameters of different interfaces and alsoto evaluate ballast breakage behaviourunder different load and interface conditions. The study was based on Indian Standard ballast gradation which is currently practiced in Sri Lanka. Shear strength and degradation of fresh ballast were compared with that of three different interfaces under three different normal loads througha series of direct shear tests using large scale direct shear test apparatus design and built at the University of Peradeniya.

2 MATERIAL AND METHODS

The tests were conducted on biotite gneiss ballast sample obtained from a stock pile of Railway Department in Gampola. The collected ballast samples were cleaned with waterto remove any dust and clay adhering to them as mentioned in Navaratnarajah & Indraratna (2017), dried before screeningthrough selected sieve sizes, and then mixed in the desiredproportions to obtain the required particle size distribution (PSD). Figure 1

shows upper and lower limits of Indian standard gradation and the gradation of prepared laboratory sample.

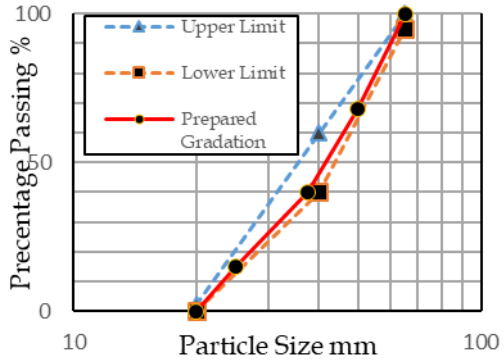

Fig. 1 Particle Size Distribution (PSD) of Ballast.

A used wooden sleeper was collected from Railway Department Gampola and cut according the large-scale shear apparatus setup(wooden sleeper was made circular in shape to fit the direct shear test apparatus) as shown in Figure 2a. Grade 60 concrete was used to make the circular concrete sleeper sample as shown in Figure 2b. 10 mm thick USP was attached to a circular concrete sleeper to make USP-ballast interface as shown in Figure 2c.

(a) (b) (c)

Fig. 2 Different interfaces with ballast (a) Wooden sleeper; (b) Concrete sleeper; and (c)USP

Large scale direct shear apparatus used in this study could accommodate a ballast aggregate specimen of diameter 400 mm and height 300 mm, and at the execution of the test, it could shear the sample into two equal halves. Based on ASTM standards, the maximum particle size for direct shear testing is limited to 0.1 of apparatus diameter. FakhimiandHosseinpour(2008) reported that for low normal stresses, this limit could be relaxed to 0.2 for cohesionless materials with minimal increase in friction angle. In this test, the maximum particle diameter of the aggregate mixture was 63 mm and the ratio of maximum particle size to the apparatus diameter is 0.16 for the test sample. Direct shear test was performed on fresh ballast and Ballast to concrete sleeper, Ballast to timber sleeper and Ballast to shock mat (USP) attached to the concrete sleeper interfaces.

The large scale direct shear apparatus used in this study is shown in Figure 3. Upper half of apparatus is fixed to a frame and lower half is free to move horizontally to obtain shear failure at the interfaces. Top loading plate is free to move horizontally. Shear displacement and vertical displacements were measured using two displacement gauges fixed to top loading plate and lover half of apparatus. Shear force was applied using hydraulic jack. Shearing rate of 4mm/min was maintained throughout the experiment. Applied shear force was measured using load cell fixed between hydraulic jack and lower half of apparatus. Two displacement gauges and load cell were connected to a data logger in order to record load deformation data automatically. Normal loads were applied using lever arm technique. Tests were performed under three normal stresses of 30 kPa, 60 kPa and 90 kPa. Specimens were sheared until a 60 mm maximum displacement corresponding to 15% shear strain is reached. Ballast breakage was calculated according to the method which was proposed by Indrarathna, et al., (2005)

(a) (b)

Fig. 3 Large scale direct shear apparatus (a) Schematic diagram; (b) A photographic view of actual apparatus

3 RESULTS AND DISCUSSION

The Figure 4 illustrates the shear stress–shear strain relationships for fresh ballast and different interfaces under different normal loads.

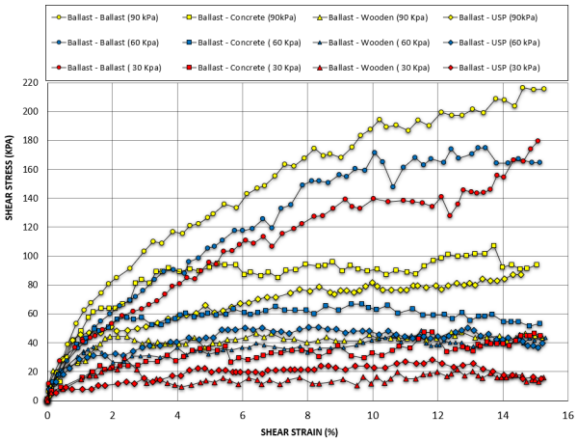

Fig. 4 Variation of Shear Stress with Shear strain for different interface conditions

The peak shear strengths occurred between 5 and 10% of strain in all fresh ballast and the particle interlocking of highly angular fresh ballast is the contributor for these peak values. In all the other interfaces, the surface friction between ballast and interface material significantly affect the stress-strain behavior and is also increases with the increase of normal stress.

Figure 5 illustrates the shear strain vs normal strain behavior of the specimens for each normal stress.Maximum dilation was occurred in fresh ballast and dilation has been increased with the decrease of normal load.

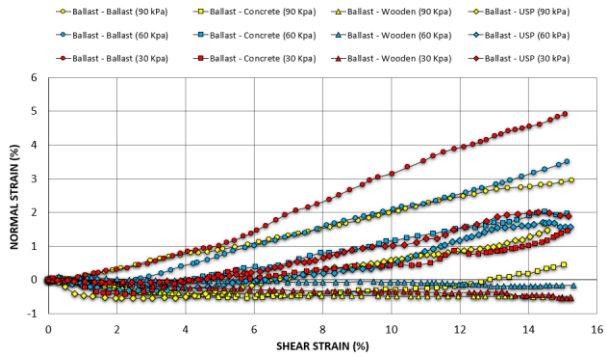

Fig. 5 Shear strain vs Normal strain behavior

Dilation has not been occurred in Ballast-Wooden interface because wood is somewhat soft compared with concrete surface therefore ballast particles will sink in to the wooden sleeper material. Then with the application of shear stress ballast will shift on the wooden plane and there may not be any particle rolling on the surface. Then with the application of shear stress surface will be damaged and only volume reduction can be noticed. The photographs of wooden sleeper before and after the test are shown in Figures 6a and b, respectively

(a) (b)

Fig. 6 Wooden sleeper (a) before the test; (b) after the test

Concrete surface is relatively hard then ballast particle will be rolled in the concrete surface therefore dilation has been occurred in ballast-concrete interface. Concrete sleeper has not damaged much. The photographs of concrete sleeper before and after the test are shown in Figures 7a and b, respectively.

(a) (b)

Fig. 7 Concrete Sleeper (a) Before Test; (b) After Test

USP is a composite material it is also soft but will not easily damaged like wooden surface. The shear resistance of the USP also relatively larger than wodden sleeper.There were no any damaged observed on USP surface after the test performed. Hence particle rolling may be occurred on USP surface and dilation has been occurred from the results shown in Figure 5. The photographs ofUSP before and after the test are shown in Figures 8 a and b, respectively.

(a) (b)

Fig. 8 USP (a) Before Test; (b) After Test

Figure 9 shows shear stress to normal stress relationship at peak and the resulting Mohr– Coulomb (MC) failure surface assuming zero cohesion for ballast and interface materials. Table 1 shows the value of friction angle for fresh ballast and for the interfaces tested in this study.

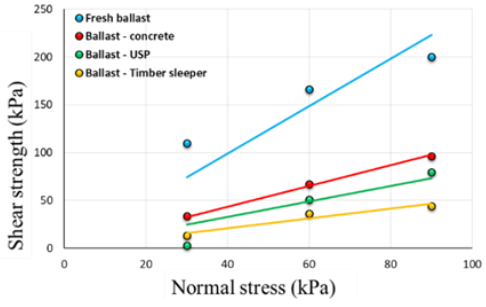

Fig. 9 Peak shear stress-normal stress relationship

Table 1. Friction angles of different interfaces

Material/Interface	Friction Angle (ϕ)
Fresh Ballast	68.6°
Ballast-Concrete	47.3°
Ballast-USP	39.2°
Ballast-Wooden	36.1°

After each test ballast samples were sieved again to obtain ballast breakage. Ballast breakages were calculated using the method proposed by Indraratna, et al., (2005). Figure 9 shows the calculated ballast breakage index values.

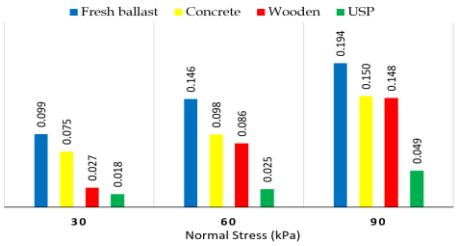

Fig. 10 Ballast Breakage Index values

Ballast breakage has increased with the increase of normal load. Highest breakage was occurred in fresh ballast and lowest is occurred in Ballast-USP interface. USP is soft material therefore breakage is low. Ballast-Concrete interface has comparatively higher breakage than Ballast-Wooden interface because of the harder interface.

4 CONCLUSION

Large scale direct shear test have been conducted for ballast and some of selected interfaces of rail track foundation. Ballast has highest shear strength because of the particles are highly angular in nature and the strength of parent material is high. ballast–concrete interface has high shear strength. Lowest shear strength is occurred in ballast–wooden interface. ballast–USP interface has high shear strength than ballast–wooden interface. Highest breakage was occurred in fresh ballast and lowest is occurred in ballast-USP interface. USP is soft material therefore breakage is low in USP. ballast-concrete interface has comparatively high breakage than ballast-wooden interface. Using concrete sleeper will give high lateral resistance than using wooden sleeper. However, ballast breakage is high in concrete sleeper. Introducing USP with the concrete sleeper significantly reduce the ballast breakages. Therefore, the life cycle of ballast materials can be increased by introducing rubber elements such as USPs to the concrete sleepers.

ACKNOWLEDGMENTS

The financial support for this project was provided by University of Peradeniya Research Grant (URG/2017/29/E) is greatly appreciated. We would like to pay our gratitude to Eng. Sirisena, Faculty Workshop Engineer and the technical staffs of the Engineering workshop for helping to build the large-scale shear apparatus. Geotechnical laboratory and staffs of Gampola railway unit staffs for helping us getting the test materials and helping in many ways completing this project is also appreciated.

REFERENCES

Abadi, T., Pen, L. L., Zervos, A. &Powrie, W., n.d. Measuring the Area and Number of Ballast Particle Contacts at Sleeper/Ballast and Ballast/Subgrade Interfaces.

Dissanayake, D., Kurukulasuriya, L. & Dissanayake, P., 2016. Evaluation of shear strength parameters of rail track ballast in Sri Lanka. Journal of the National Science Foundation of Sri Lanka, Volume 44, pp. 61-67.

Dissanayake, G., Kurukulasuriya, L. & Dissanayake, P., 2014. Direct Shear Testing of Rail Track Ballast Using a Large Scale Direct Shear Apparatus. ICSBE.

Fakhimi, A. &Hosseinpour, H., 2008. The role of oversize particles on the shear strength and deformational. American Rock Mechanics Association.

Indrarathna, B., Lackenby, J. & Christie, D., 2005. Effect of confining pressure on the degradation of ballast under cyclic loading. Geotechnique, Volume 55, p. 325–328.

Indraratna, B. et al., 2014. Use of shock mats for mitigating degradation of railroad ballast. Sri Lankan Geotechnical Journal, Volume 6, pp. 32-41.

Navaratnarajah, S. K., Indraratna, B. &Nimbalkar, S., 2015. Performance of rail ballast stabilized with resilient rubber pads under cyclic and impact loading. ICGEColombo2015, pp. 617-620.

Navaratnarajah, S. K. & Indraratna, B. (2017) Use of Rubber Mats to Improve the Deformation and Degradation Behavior of Rail Ballast under Cyclic Loading, ASCE Journal of Geotechnical and Geoenvironmental Engineering, 143 (6), p. 04017015.

Navaratnarajah, S. K., Indraratna, B. & Ngo, N. T. (2018) Influence of Under Sleeper Pads on Ballast Behavior Under Cyclic Loading: Experimental and Numerical Studies, ASCE Journal of Geotechnical and Geoenvironmental Engineering, 144 (9), p. 04018068.

Suiker, A. S. J., Selig, E. T. & Frenkel, R., 2005. Static and Cyclic Triaxial Testing of Ballast and Subballast. Journal of Geotechnical and Geoenvironmental Engineering, 131(6).

Profillidis, V. A. 2014. Railway management and engineering, ashgate publishing, ltd.